Materials Today Chemistry 12 (2019) 266–281

Contents lists available at ScienceDirect

Materials Today Chemistry

journal homepage: www.journals.elsevier.com/materials-today-chemistry/

Incorporation of rare earth elements with transition metal–based materials for electrocatalysis: a review for recent progress

W. Gao [a, b, c], D. Wen [c], J.C. Ho [b, *], Y. Qu [a, **]

[a] Center for Applied Chemical Research, Frontier Institute of Science and Technology, And State Key Laboratory for Mechanical Behavior of Materials, Xi'an Jiaotong University, Xi'an 710049, PR China
[b] Department of Materials Science and Engineering, City University of Hong Kong, 83 Tat Chee Avenue, Kowloon, Hong Kong SAR
[c] State Key Laboratory of Solidification Processing, Center for Nano Energy Materials, School of Materials Science and Engineering, Northwestern Polytechnical University and Shaanxi Joint Laboratory of Graphene (NPU), Xi'an 710072, PR China

ARTICLE INFO

Article history:
Received 12 December 2018
Received in revised form
6 February 2019
Accepted 7 February 2019

Keywords:
Electrocatalysts
Energy conversion
Electrochemical reactions
Modifications

ABSTRACT

Improving the catalytic activity of various electrocatalysts is of significant importance for the efficient conversion between electricity and chemical energy for sustainable developments. Lately, modification of transition metal–based electrocatalysts with foreign elements is growing rapidly, and rare earth (RE) elements are of particular interest among various elements because of their special structural features. Here, in this review, we perform a comprehensive survey on the recent progress in RE element –incorporated electrocatalysts for various electrochemical reactions, including hydrogen evolution, oxygen evolution, oxygen reduction, and methanol oxidation reactions. As benefited from the RE incorporation, the structural and catalytic property changes of host electrocatalysts are summarized for different reactions, in which it is evident that there are many positive promotions induced from RE elements for the enhanced electrocatalysis. Several important insights are also discussed to further our knowledge of integrating RE elements to improve associated electrocatalytic properties of the catalysts investigated. The final section describes the challenges for the design, structural optimization, mechanistic investigation, and technological applications for the RE element–incorporated electrocatalysts and concludes with an outlook on the future development of these catalysts for energy conversion and storage.

1. Introduction

Over the past several decades, transition metal–based materials, including those based on non-precious metals and precious metals, have been broadly researched as heterogeneous catalysts for various electrocatalytic reactions, such as hydrogen evolution, oxygen evolution, oxygen reduction, methanol oxidation, and so on, to realize efficient energy conversion *via* electrocatalysis pathways for sustainable society. However, their catalytic performances are still not satisfactory to meet the requirement of future applications and are the bottlenecks for highly active electrocatalytic processes. Modification of catalysts with foreign elements and their compounds has been generally accepted as a reliable approach to modulate their intrinsic structures, surface properties, and catalytic performances, and significant efforts have been devoted to this field recently. Not only catalytically active transition metals including Mn, Fe, Co, Cu, and so on [1–6] but also inactive ones such as Ti, V, Cr, and Zn [7–10], are adopted as dopants, additives, and sensitizers, and cocatalysts have been extensively explored to regulate the catalytic properties of transition metal–based electrocatalysts, as reported by previous reports.

Rare earth (RE) elements, consisting of Sc, Y, and other 15 lanthanide elements, have been applied in the fields of optics, electromagnetics, electronics, and heterogeneous catalysis. The application of RE elements in electrocatalysis started as early as the 1970s, when the alloy of $LaNi_5$ was first demonstrated as a cathode material for hydrogen evolution reaction (HER) in alkaline solution by Miles [11]. However, research on RE element–incorporated materials was not growing as fast as expected, although rare and limited reports were proposed during the last century [12,13]. Although not being the focus for electrocatalysis in the 20th

* Corresponding author.
** Corresponding author.
E-mail addresses: johnnyho@cityu.edu.hk (J.C. Ho), yongquan@xjtu.edu.cn (Y. Qu).

https://doi.org/10.1016/j.mtchem.2019.02.002
2468-5194/

century, RE elements have been drawing increasing attention in electrocatalysis since the 2000s by modulating and enhancing the catalytic properties of various transition metal–based electrocatalysts to push forward the progress of electrocatalysis. Especially, with the development and assistance of nanoscience and nanotechnology, recent advances exhibit the broad applications of RE element–incorporated electrocatalysts in various electrocatalytic fields, including HER, oxygen evolution reaction (OER), oxygen reduction reaction (ORR), methanol oxidation reaction (MOR), and other reactions, but a summary to survey the development, mechanism, and applications of RE element–incorporated electrocatalysts is still lacking. It is worth mentioning that the perovskite with the general ABX_3 formula, is a typical family of RE element–incorporated structures and usually has different RE elements to function as A-site cations, such as $LaCoO_3$. Because RE element–incorporated perovskites have been widely studied and summarized in photoelectrocatalysis, electrocatalysis, and other heterogeneous catalysis, we will focus on the non-perovskite-structured, transition metal–based materials with RE element incorporation and RE element–based compounds to summarize their recent advances and developments in this review.

Herein, several parts will be described in this review, including (1) the fundamental knowledge about RE elements and different methods of incorporating RE elements with other transition metal–based electrocatalysts, (2) the applications of RE element–incorporated electrocatalysts in various electrocatalytic reactions (namely, HER, OER, ORR, MOR, and so on) and their possible mechanisms on promoted catalytic properties from RE element incorporation, and (3) a summary of recent developments and perspectives of RE element–incorporated electrocatalysts for future challenges.

2. RE elements and RE element–incorporated electrocatalysts

RE elements are consisted of a set of 17 elements, namely, Sc, Y, and other 15 lanthanide elements of La, Ce, Pr, Nd, Pm (which is not generally researched in catalysis because of its radioactivity), Sm, Eu, Gd, Tb, Dy, Ho, Er, Tm, Yb, and Lu with 4f orbitals (Fig. 1). Sc and Y, located in the IIIB group of the periodic table of elements, as well as lanthanide elements with the 4f orbital have larger atomic and ionic radii than other transition metals such as Mn, Fe, Co, and Ni. All RE elements have stable RE^{3+} chemical states whereas some of them have tetravalent states such as Ce^{4+} and Tb^{4+}. Because of the increase in 4f electrons and the corresponding lanthanide contraction effect leading to the similar electronic structures as well as gradual changes in ionic radii for lanthanide elements, there are many similarities in physical and chemical properties, but also differences in optical, magnetic, and catalytic properties.

For transition metal–based electrocatalysts, the integration or incorporation with RE elements started with $LaNi_5$ in the 1970s, and they are developing fast in the 21st century. Not only non-precious metals including Co, Ni, and Fe but also precious metals such as Pt, Au, and Pd realized the incorporation with RE elements to be exploited in electrocatalytic reactions. Particularly, Ce and its oxide, cerium oxide (CeO_2 or ceria), attracted special interest in electrocatalysis because of their quick transfer between Ce^{3+}/Ce^{4+} redox pairs, the details of which will be discussed in the following sections. To have a better understanding on the application of RE elements, we will mainly focus on four typical electrocatalytic reactions, namely, HER, OER, ORR, and MOR, to summarize the features and roles of RE elements.

Preparing RE element–incorporated electrocatalysts can be realized by different physical and chemical methods, including high-temperature melting (such as arc melting and induction melting), magnetron sputtering, wet chemical deposition, and electrodeposition. As a result of various preparation methods for RE element–incorporated electrocatalysts, three of them have been proposed to realize the collaboration between RE elements and other electrocatalysts for non-perovskite structures: (1) forming alloys with other metals to obtain new crystalline-structured alloys, such as $LaNi_5$ and Pt_5Gd; (2) doping RE element ions into host materials during the preparation, such as doping Ce^{3+} into NiFe-layered double hydroxide (LDH) nanosheets; and (3) building heterogeneous structures between electrocatalysts and RE element–based compounds, for example, the formation of interface between Ni and CeO_2. The high-temperature melting method is generally used for the mass preparation of bulk alloys with a wide range of RE contents [12], whereas the magnetron sputtering can effectively synthesize alloy nanoparticles with well-controlled size, but it is not suitable for mass production [14]. The chemical and electrochemical deposition methods, such as doping RE element ions into host materials and building heterogeneous structures with other nanostructured electrocatalysts are widely used because of their facile apparatus and low costs to prepare the morphology-controlled nanomaterials. It is worth mentioning that because of the huge difference in atomic radius between RE elements and other transition metals, the doping of RE element ions into other electrocatalysts is not easy, and instead, it often results in the formation of RE element–based compounds. In this regard, different approaches to combine RE elements and other metals are then expected for the further design and preparation of RE element–incorporated electrocatalysts.

3. RE element–incorporated electrocatalysts for HER

Hydrogen evolution is an important half reaction for both water electrolysis in acidic and basic media and chloralkali process in alkaline solution. HER generally involves two processes, namely, the Volmer–Tafel path and Volmer–Heyrovsky path [15]. Besides noble metals such as Pt, other 3d and 4d transition metal–based materials have also been extensively investigated as cathodic electrocatalysts in different electrolytes.

3.1. Alloying with different RE elements for HER

In the 20th century, transition metal alloys with d-orbital metals are widely studied as cathode materials to replace pure metal electrodes for HER in alkaline solutions because of their low cost, improved anticorrosion property, and activity. However, how to design stable and catalytically active electrocatalysts was the challenge. According to the Brewer–Engel theory, whenever metals of the left half of the transition series that have empty or half-filled vacant d orbitals are alloyed with metals of the right half of the transition series that do not have internally paired d electrons available for bonding in the pure metal, there arises well-pronounced synergism in electrocatalysis for HER, which often exceeds individual effects of precious metals on each other (the synergism condition) and approaches the reversible behavior within the wide range of current density [16]. Therefore, the combination of left-half transition metals of light RE elements (such as Sc, Y, La, Ce, and Pr) with other right-half transition metals (such as Fe, Co, and Ni) would lead to more active alloys than their single metal counterparts for electrocatalytic hydrogen evolution. With the prediction of the Brewer–Engel theory, $LaNi_5$ would be one of the upmost electrocatalytic active alloy structures with the intermetallic phase of highest symmetry and minimum entropy for HER. As a striking hydrogen storage material, $LaNi_5$ was first reported as electrocatalysts for HER by Miles [11] in 1975. Later, $LaNi_5$ and $MmNi_5$ (mischmetal) were specifically researched by Tamura et al. [12,13]

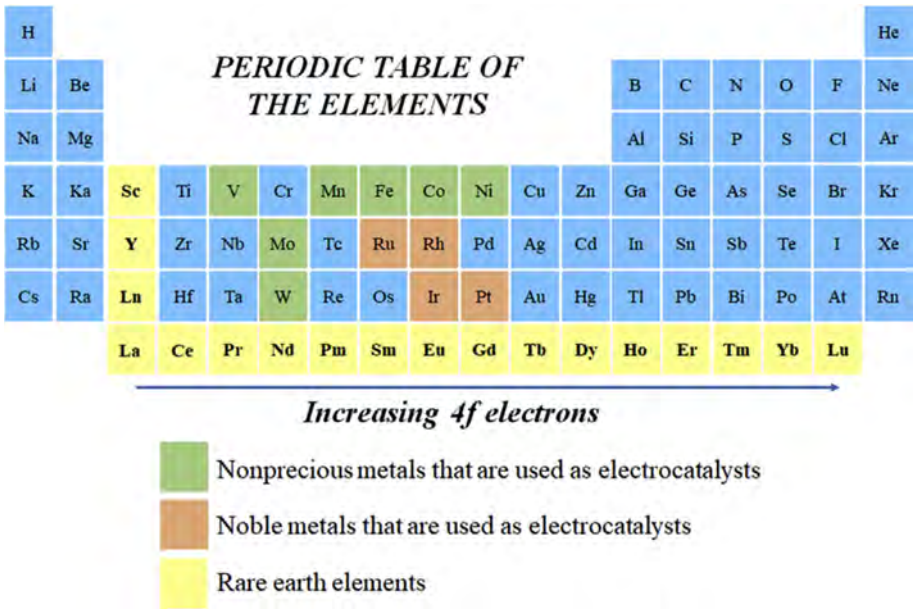

Fig. 1. Elements that are used for electrocatalysis and rare earth elements.

for electrocatalytic hydrogen production and exhibited better performance in alkaline solution than pure Ni. For Ni-based alloys, a series of studies on the effect of various RE elements such as Y, Ce, Pr, Sm, and Dy with low contents (usually <10 at%) are proposed and demonstrated to investigate their contributions in the activity for HER [17–19]. Recently, introducing RE elements and other transition metals such as Fe, Zn, Mo, and Pt to fabricate crystalline alloys is also realized to improve their activity in alkaline water electrolysis [20–23]. From this aspect, using light RE elements (namely, from La to Gd in the lanthanide series) with empty and vacant d orbitals are favored to incorporate with catalytically active elements of Fe, Co, and Ni with half-filled 3d orbitals to synthesize crystalline alloys.

3.2. Incorporation with Ce ion and CeO_2 for HER

The strategy of alloying with other metals using RE elements is not the only pathway to improve the catalytic property of transition metals, but different methods of doping RE element ions and incorporating with RE element oxides are developed in the past decade. In specific, Ce and its oxide, cerium oxide, are among the most attractive candidates to incorporate with transition metals, *via* the strategies of doping Ce ions and synthesizing composites with ceria. For instance, adding microsized and nanosized CeO_2 particles onto electrodes during the electrodeposition of Ni-based electrocatalysts was reported as a novel approach to modify the intrinsic structural property of electrocatalysts [24–26]. With the help of ceria, Zheng et al. [24] demonstrated the modified microstructure of the Ni electrode with more uniform grain and less internal stress, leading to the better catalytic activity and charge transfer property. Moreover, further investigations have suggested that the concentration of ceria can regulate the content of sulfur in Ni–S–coated layers to further tune their activity toward alkaline HER [25,26]. Adding ceria into the suspensions for the electrodeposition method can also improve the crystallinity of the Co–W alloy, as exhibited by Sheng et al. [27], in which the crystalline Co–W/CeO_2 composites performed enhanced activity for HER compared with the amorphous Co–W alloy.

Although ceria has been reported as an effective additive for the electrodeposition of transition metal alloys, its influence on the catalytic process for HER requires further clarification. Recently, Weng et al. [28] unveiled the role of ceria on the Ni/CeO_2 interfaces using experimental investigation and density functional theory (DFT) calculations. Carbon nanotubes (CNTs) are used to anchor the Ni/CeO_2 heterogeneous structure (Fig. 2a) and conductivity, while the Ni/CeO_2 interfaces promoted the water dissociation and benefited the lower hydrogen binding energy to improve HER activity with smaller overpotential (Fig. 2b). The DFT result depicted the lower energy for water dissociation on the Ni_1/CeO_2 (111) interface compared with that of pure Ni(111), illustrating the easier formation of H* intermediates on the surface of Ni/CeO_2 (Fig. 2c). The subsequent analysis showed the lower hydrogen binding energy on the Ni_1/CeO_2 (111) interface to accelerate the conversion of H* intermediate into H_2 (Fig. 2d). Therefore, constructing such an interface between the metal and metal oxide (herein, ceria) can facilitate the breaking of H–OH bond to form H* intermediates and optimize the hydrogen binding strength to lower the H_2 adsorption energy.

Lately, various interfaces between CeO_2 (or CeO_x) and transition metal–based electrocatalysts , including CoP-CeO_2 [29], Ni_2P-CeO_2 [30], CoP-CeO_2-C [31], Ni_3N-CeO_2 [32], and NiFe-LDH-CeO_x [33], are constructed to improve their catalytic activity for both acidic and alkaline hydrogen evolution, as exhibited in Fig. 3. In both acidic and alkaline media, the hydrogen adsorption energy would be lower, whereas the water dissociation process to produce H* intermediates would be easier with the assistance of CeO_2 in alkaline solution, which results in faster turnover of the optimally absorbed intermediates to generate hydrogen molecules [29,31]. Typically, Zhang et al. [29] reported the significant decrease in overpotential for CoP–CeO_2/Ti mesh compared with that for CoP/Ti mesh for hydrogen evolution in basic solution (Fig. 3a) because of the decreased water adsorption and optimal hydrogen adsorption free energies. Similarly, Sun et al. [32] demonstrated the decrease in overpotential for Ni_3N catalyst with CeO_2 incorporation toward alkaline HER (Fig. 3b). Impressively, with the decoration of oxygen vacancy–rich CeO_x nanoparticles, the strong local electronic interaction between NiFe-LDH nanosheets and CeO_x led to the enhanced activity for both HER and OER, further contributing to a low potential of 1.51 V to drive the current density of 10 mA cm^{-2} for overall water splitting (Fig. 3c), as exhibited by Wang et al. [33].

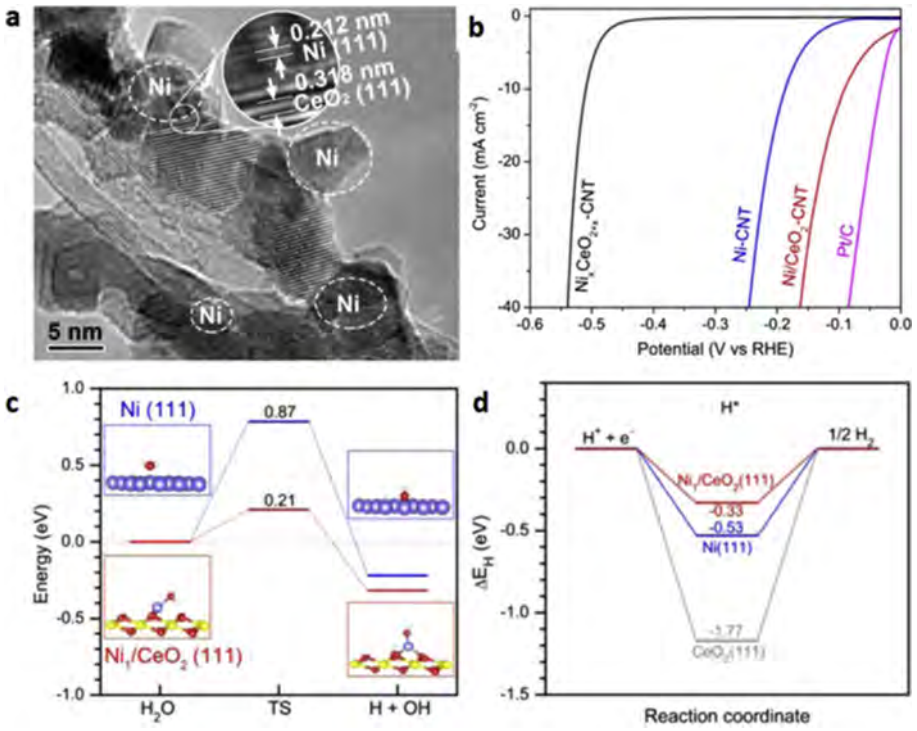

Fig. 2. (a) High-resolution TEM image of Ni/CeO_2 CNT. (b) Polarization curves of Ni/CeO_2 CNT, Ni_xCeO_{2+x} CNT, Ni CNT, and commercial Pt/C in 1 M KOH solution. (c) DFT-calculated reaction energy diagram of water dissociation for $Ni_1/CeO_2(111)$ and Ni(111). (d) DFT-calculated HBE for $Ni_1/CeO_2(111)$, Ni(111), and $CeO_2(111)$ systems. Reproduced with permission from Ref. [28]. Copyright 2015, American Chemical Society. CNT, carbon nanotube; DFT, density functional theory; TEM, transmission electron microscopy; HBE, hydrogen binding energy.

Using ceria as the substrate to incorporate with metals and metal oxides is also feasible to improve the activity of electrocatalysts. For example, Demir et al. reported the superior catalytic activity of nanoceria-supported Ru nanoparticles for HER in acid. With a low content of Ru, this catalyst exhibited small onset potential and overpotential to achieve efficient hydrogen generation [34]. Moreover, Long et al. demonstrated the positive effects of ceria layers as the substrate to support other metal oxides and metals by accelerating the dissociation of water molecules and strong electron interactions between ceria and transition metals as well as their oxides to promote both HER and OER processes, where very small overpotentials are required to fulfill efficient HER, OER, and overall water splitting [35].

Doping Ce^{3+} ions into CoP is a recently developed novel method by our group to tune the electronic structure of CoP for efficient HER in both acidic and alkaline solutions [36]. Theoretical calculations by DFT demonstrated the lower hydrogen adsorption free energy on different CoP facets after introducing Ce (Fig. 4a), whereas Bader charge analyses revealed the modulated electronic structure of Co with negatively charged state by Ce doping. Experimental results witnessed the doping of Ce into CoP (Fig. 4b), whereas polarization curves came into agreement with those of theoretical analyses that significant decreases in overpotentials and Tafel slopes are observed in both acidic and alkaline electrolytes for HER (Fig. 4c and d), suggesting the method of doping Ce can greatly benefit the electronic structure of host materials to promote their activity toward HER.

3.3. Other RE element–incorporated electrocatalysts for HER

Besides Ce-based species, other RE elements can also promote the activity of catalytically active species for HER. For example, Liu et al. [37] revealed the promotion for Ru as the catalyst for alkaline HER by introducing amorphous $Y(OH)_3$ nanosheets as the scaffold to build Ru/$Y(OH)_3$ hybrids. Amorphous $Y(OH)_3$ with abundant structural defects and coordination-unsaturated atoms provided rich nucleation sites for the formation of highly dispersed ultrafine Ru nanoparticles, as well as enabled the strong interaction between Ru and its nanoparticles, leading to better water dissociation kinetics and structural stability.

Comparisons of pristine electrocatalysts and their corresponding RE element–incorporated ones in catalytic performances for HER are summarized in Table 1. Thus, from previous research outcomes, the enhanced activity for HER by RE element incorporation is mainly contributed to modulate the electronic structures of hosts and facilitate the water dissociation to generate active H* species. Three methods are generally adopted to prepare RE element–incorporated electrocatalysts and their derivatives for enhanced HER: (1) alloying with other transition metals, (2) applying RE element oxides and hydroxides as substrates and additives to build microinterfaces and nanointerfaces of transition metals and their derivatives/RE element oxides (especially CeO_2), and (3) doping RE element ions into the hosts of transition metal–based electrocatalysts.

4. RE element–incorporated electrocatalysts for OER

As is known to all, OER is a more sluggish and complex half reaction with a two-electron or four-electron process to convert water into oxygen molecules [38]. For a typical four-electron process, the transfer and conversion of various oxygen-involving intermediates and the release of produced oxygen molecules are related to the reacting rate, from the viewpoint of kinetics. Therefore, catalysts with optimal binding strength with intermediates

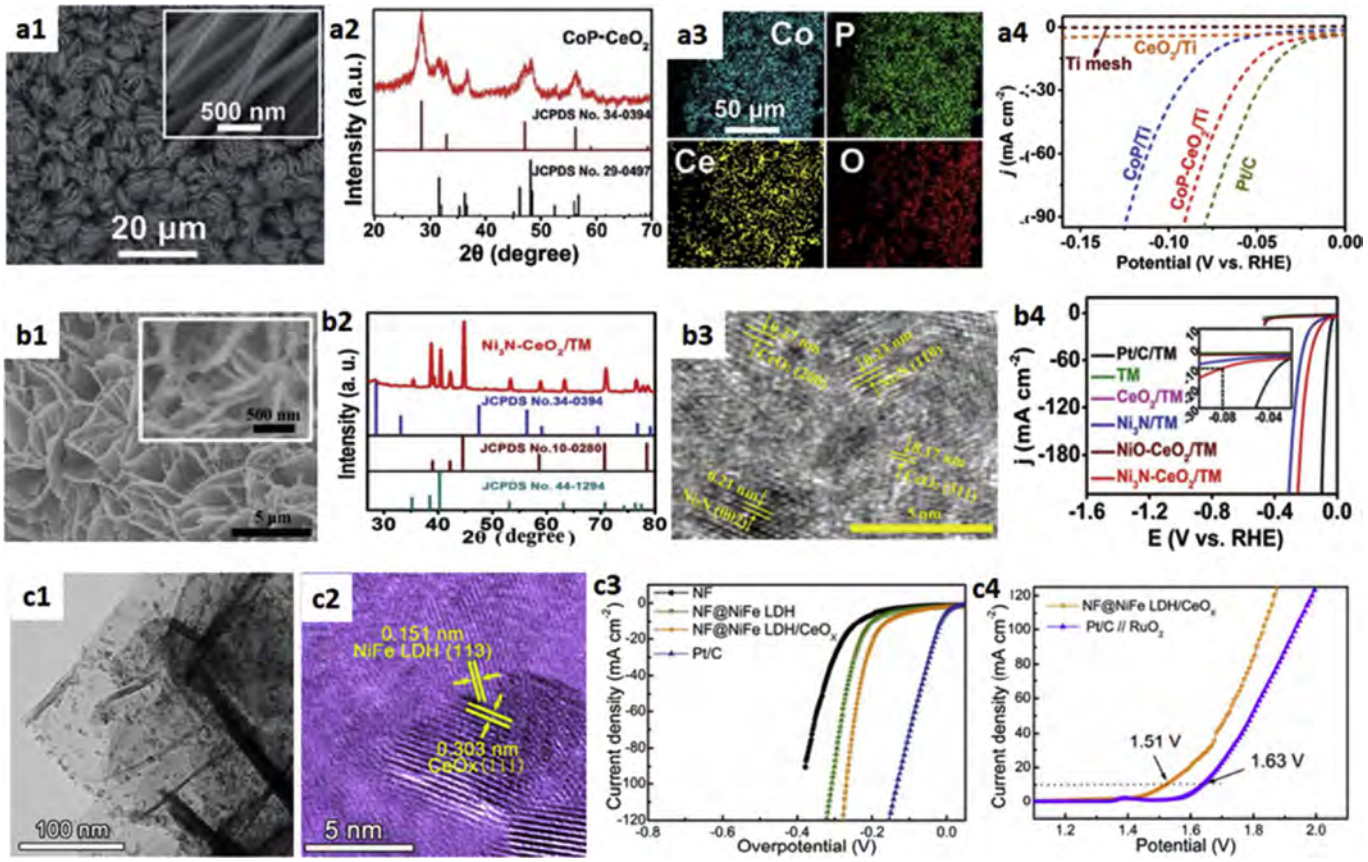

Fig. 3. (a1) SEM image and (a2) XRD patterns of CoP–CeO_2 scratched down from Ti mesh. (a3) EDX elemental mapping of Co, P, Ce, and O for CoP–CeO_2/Ti. (a4) Polarization curves of Ti mesh, CeO_2/Ti, CoP/Ti, CoP–CeO_2/Ti, and Pt/C on Ti mesh for the HER at a scan rate of 2 mV s^{-1}. Reproduced with permission from Ref. [29]. Copyright 2018, Royal Society of Chemistry. (b1) SEM image, (b2) XRD pattern, and (b3) HRTEM image of Ni_3N–CeO_2. (b4) LSV curves of HER for bare TM, Pt/C/TM, CeO_2/TM, Ni_3N/TM, NiO–CeO_2/TM, and Ni_3N–CeO_2/TM (the inset shows the LSV curves of the HER in the low current density range) (iR corrections). Reproduced with permission from Ref. [32]. Copyright 2018, Royal Society of Chemistry. (c1) TEM image and (c2) HRTEM image of NF@NiFe-LDH/CeO_x. (c3) Linear sweep voltammetry curves toward HER of NF, NF@NiFe-LDH, NF@NiFe-LDH/CeOx, and Pt/C in 1.0 M KOH solution at a scan rate of 5 mV s^{-1} with iR correction. (c4) Linear sweep voltammetry curves of electrolysis for NF@NiFe-LDH/CeO_x and Pt/C–RuO_2 with a scan rate of 5 mV s^{-1} in 1.0 M KOH aqueous solution without iR correction. Reproduced with permission from Ref. [33]. Copyright 2018, American Chemical Society. HER, hydrogen evolution reaction; LDH, layered double hydroxide; SEM, scanning electron microscopy; TEM, transmission electron microscopy; XRD, X-ray diffraction; EDX, energy dispersive X-ray spectroscopy; HRTEM, high-resolution transmission electron microscopy; LSV, linear sweep voltammetry; TM, Ti mesh; RHE, reversible hydrogen electrode.

and enhanced oxygen mobility would be favored for oxygen-involved reactions, including both OER and ORR. The application of RE elements in ORR will be described in the following section, and herein, we will focus on the incorporation of RE elements with transition metal–based electrocatalysts for OER.

4.1. Doping Ce ion into electrocatalysts for OER

Doping Ce ions into transition metal–based electrocatalysts is also a feasible approach to modulate their property for OER. Typically, Ng et al. [39] demonstrated the significant enhancement of the OER activity of electrodeposited NiO_x with Ce as the dopant from the combination of experimental observations and theoretical analyses. By regulating the Ni:Ce ratio, the optimized electrocatalysts of $NiCeO_x$ supported on Au substrates exhibited greatly improved activity (Fig. 5a), whereas DFT calculations revealed that the existence of Ce in the vicinity of undercoordinated Ni edge on NiOOH $(01\bar{1}2)$ contributed to lower theoretical overpotential (Fig. 5b). Moreover, because of the strong electronic interaction between Ce and Ni and the good oxophilicity of Ce, the OER energy descriptor ΔG_O-ΔG_{OH} also lowered to an optimized value for OER. Lately, Xu et al. [40] reported better OER activity of Ce-doped NiFe-LDH/CNTs than that of pure NiFe-LDH/CNT counterparts (Fig. 5c and d). Several factors of introducing Ce are ascribed to the improvement for NiFe-LDH. First, the formation of the eight-fold dodecahedron or nine-fold monocapped square antiprism coordination layers after doping Ce resulted in the change in layer composition and coordination structure of LDH. Second, Ce^{3+} (and Ce^{4+}) doping led to more lattice distortion and imperfections of active sites for OER. Third, more oxygen vacancies as the result of increasing defects and the fast, intrinsic Ce^{3+}/Ce^{4+} redox transformation contributed to a rapid diffusion of oxygen through short ion diffusion paths and the dynamics of the released oxygen in the lattice. Therefore, the aforementioned research introduces the positive effects of doping Ce ions into hosts to promote the electronic interactions and create a more defective structure for OER.

4.2. Incorporation with CeO_2 for OER

Compared with Ce ions, the oxide CeO_2 is extensively considered for OER as the additive to promote the activity and stability. Generally, ceria, especially with rich defects, is favored for heterogeneous catalysis because of the abundant active sites and oxygen storage ability for buffering oxygen species [41]. Although ceria itself is not catalytically active for oxygen-involved reactions such as OER or ORR, it can function as the cocatalyst to benefit the host electrodes, which has been proposed and proved by many recent literature studies. Several typical results are described here to learn the

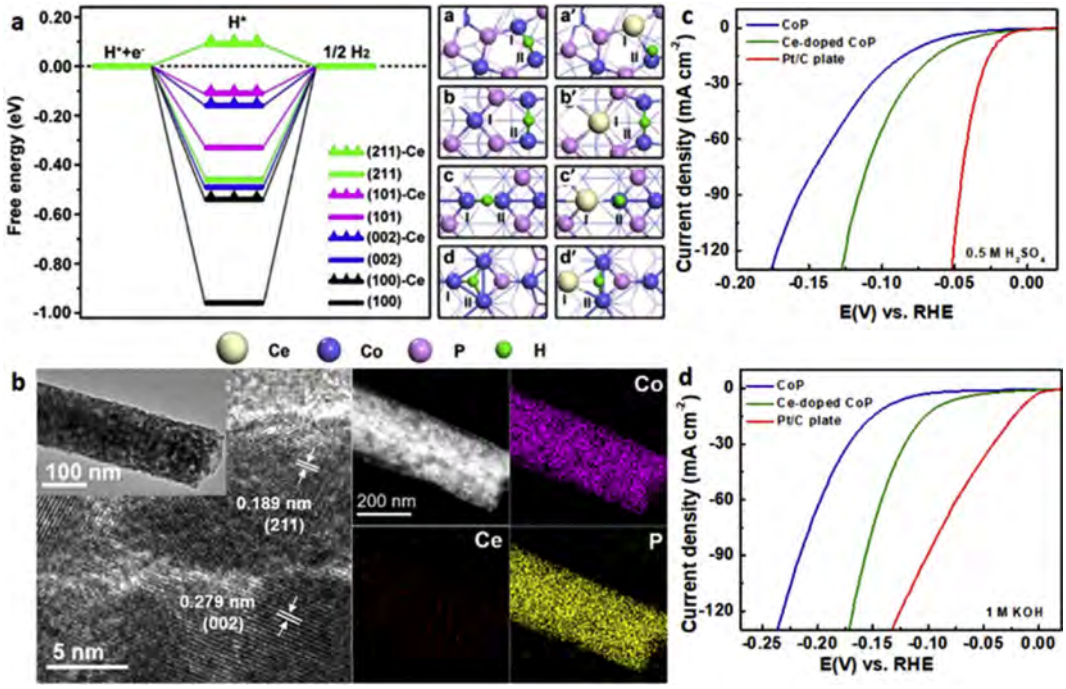

Fig. 4. (a) Calculated free energy diagram for HER on different facets of CoP and Ce-doped CoP with optimized adsorption structures of H*. (b) TEM and HRTEM images of Ce-doped CoP nanowires, DF-TEM images of Ce-doped CoP, and element mapping images of Co, Ce, and P. Polarization curves (with iR corrections) of CoP, Ce-doped CoP, and Pt/C catalysts with a scan rate of 5 mV/s in (c) 0.5 M H_2SO_4 and (d) 1 M KOH solutions. Reproduced with permission from Ref. [36]. Copyright 2017, Elsevier Inc. HER, hydrogen evolution reaction; TEM, transmission electron microscopy; HRTEM, high-resolution transmission electron microscopy; DF-TEM, dark-field transmission electron microscopy; RHE, reversible hydrogen electrode.

Table 1
Summary of the HER catalytic property of various electrocatalysts before and after RE element incorporation.

Electrocatalysts	Overpotential @ 10 mA cm^{-2} (mV)	Tafel slope (mV dec^{-1})	Electrolyte	Ref.
Ni	~370	118	1 M NaOH	[17]
$Ni_{94}Pr_6$	~240	81		
Pt	570 (@ 100 mA cm^{-2})	130	8 M KOH	[23]
Pt–Ce	390 (@ 100 mA cm^{-2})	114		
Ni CNT	~180	N/A	1 M KOH	[28]
Ni/CeO_2 CNT	91	N/A		
CoP/Ti	70	52	1 M KOH	[29]
CoP–CeO_2/Ti	43	45		
Ni_2P/TM	131 (@20 mA cm^{-2})	113	1 M KOH	[30]
Ni_2P–CeO_2/Ti	84 (@20 mA cm^{-2})	87		
CoP–C/CC	132	82	0.5 M H_2SO_4	[31]
CeO_2–CoP–C/CC	71	53		
Ni_3N/TM	121	155	1 M KOH	[32]
Ni_3N–CeO_2/TM	80	122		
NF@NiFe-LDH	198	130	1 M KOH	[33]
NF@NiFe-LDH/CeO_x	154	101		
Ni-TMO	198	102	1 M KOH	[35]
ceria/Ni-TMO	93	69		
CoP/Ti	74	54	0.5 M H_2SO_4	[36]
Ce-doped CoP/Ti	54	59.3		
Ru	192	82	0.1 M KOH	[37]
Ru/$Y(OH)_3$	100	66		

CNT, carbon nanotube; HER, hydrogen evolution reaction; LDH, layered double hydroxide; RE, rare earth; TMO, transition metal oxide; TM, Ti mesh; CC, carbon cloth.

promotion of OER activity for various transition metal–based electrocatalysts in alkaline electrolytes [42–50]. For instance, Zheng et al. firstly demonstrated the promotion in OER activity for $CoSe_2$ nanobelts in 0.1 M KOH solution with ultrafine CeO_2 nanoparticle decoration (Fig. 6a). The significant decrease in overpotential and apparent improved stability were observed for the CeO_2/$CoSe_2$ electrocatalysts compared with pure $CoSe_2$ [42]. Feng et al. constructed the heterolayered FeOOH/CeO_2 nanotube arrays to realize efficient OER process in 1 M KOH solution (Fig. 6b), benefiting from the well-aligned heterolayered nanotube array structures as efficient diffusion paths, strong electronic interaction between FeOOH and CeO_2 to lower the adsorption free energy of various intermediates, and high oxygen storage capacitance of CeO_2 to absorb generated oxygen [43]. By loading CeO_x nanoparticles uniformly onto the metal-organic framework (MOF)–derived CoS (Fig. 6c), Xu et al. revealed the significantly boosted OER activity and stability because of the increase in defects caused by strong interaction between CeO_x and CoS and the protection of CeO_x layer to prevent the dissolution and loss of oxidized Co species in CoS (Fig. 6c) [48]. Similarly, Zhao et al. optimized the ratio between Ce and Ni during the solvothermal method to prepare the intimate $Ni(OH)_2$–CeO_2 interface to boost oxygen evolution (Fig. 6d). With the strong electronic interactions between $Ni(OH)_2$ and CeO_2 to modulate the binding strength between intermediates and catalysts during the OER process, the activity was enhanced significantly with a decrease of ~180 mV in overpotential [50]. Not only catalytic activity but also the promotion in long-term catalytic stability was improved by ceria, as demonstrated by recent studies. Ceria is famous as an effective component to protect metals and alloys from corrosion [51]. Recently, Obata and Tkanabe [52] exhibited the protection of $NiFeO_x$ from gradual deactivation because of the loss of Fe from active sites into solution by anodic coating of a CeO_x layer. Because of the permselectivity of the ceria layer, the permeation of OH^- and O_2 was allowed whereas the diffusion of redox ions such as Fe^{3+} was hindered, preventing the inner layer of $NiFeO_x$ from corrosion and destruction. Thus, with CeO_x working as the selective

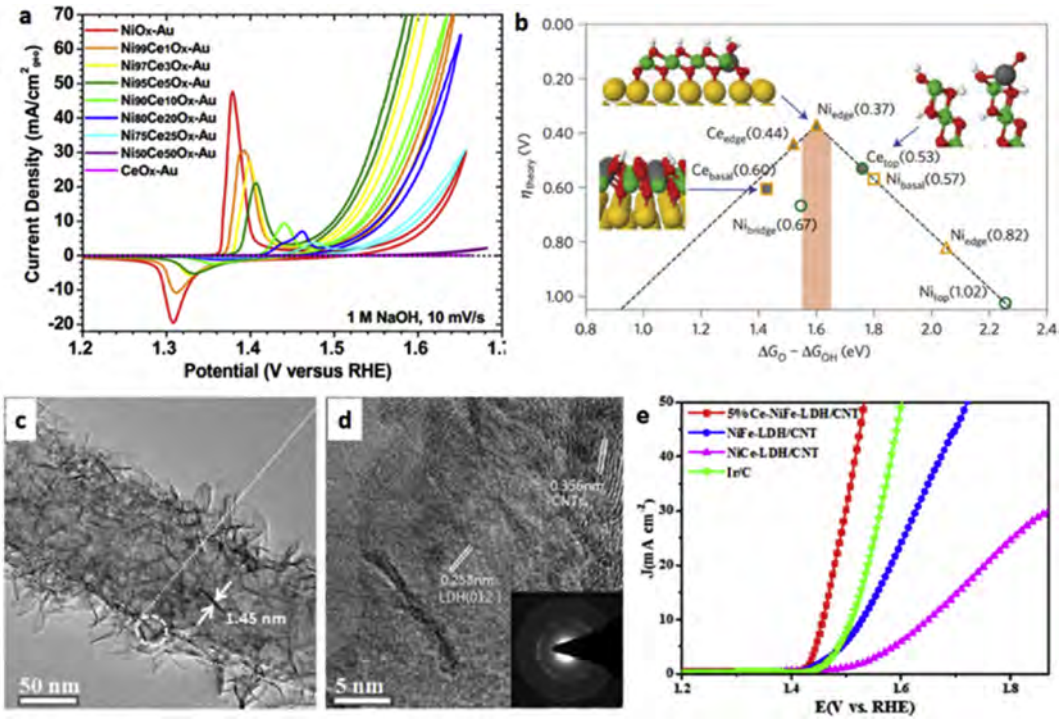

Fig. 5. (a) Cyclic voltammograms displaying the OER performance of $Ni_{1-x}Ce_xO_y$-Au catalysts. (b) Representation of the theoretical overpotential as a function of the difference in O*and HO* adsorption Gibbs energies. Green circles, gold squares, and gold triangles refer to the NiOOH (01$\bar{2}$) surface, infinite NiO_x-Au thin films, and finite NiO_x-Au thin films, respectively. Grey-filled markers indicate Ce-doped structures. Reproduced with permission from Ref. [39]. Copyright 2016, Macmillan Publishers Limited, part of Springer Nature. (c) TEM images and (d) HRTEM images of 5.0% Ce–NiFe-LDH/CNT. (e) LSV curves of 5.0% Ce–NiFe-LDH/CNT, NiFe-LDH/CNT, NiCe-LDH/CNT, and Ir/C catalysts for the OER. Reproduced with permission from Ref. [40]. Copyright 2018, American Chemical Society. CNT, carbon nanotube; LDH, layered double hydroxide; OER, oxygen evolution reaction; TEM, transmission electron microscopy; LSV, linear sweep voltammetry; HRTEM, high-resolution transmission electron microscopy; RHE, reversible hydrogen electrode.

O_2-evolving layer, both the catalytic activity and stability of as-synthesized $NiFeO_x$ are well preserved for OER.

Great efforts and achievements have illustrated and demonstrated the effect of interactions between ceria and other transition metal electrocatalyst hosts for promoting OER activity. However, rare investigations are carried out on the influences of the structural feature and intrinsic property of ceria itself to the catalytic activity. Lately, our group presented an insight into the effect of ceria structural property on the OER performance [49]. By designing two ceria-incorporated NiO electrocatalysts with various ceria distributions and configurations, their structures were analyzed and linked to their OER activity. The results showed that the embedding structure of ceria into NiO contributed to higher catalytic activity for OER than the surface-loading structure of ceria. Further exploration revealed that low coordination, ultrasmall size, and embedding of ceria, as well as Ce^{3+} doping properties of ceria, in the embedding structure can strongly affect the intrinsic property of NiO, which made it outperform the structure of loading ceria on the surface of NiO. Therefore, our work uncovered a further insight into designing electrocatalysts with different spatial configurations and the effects of structural features of ceria for the enhanced OER catalytic properties.

It should be mentioned that the properties of high oxygen storage capacity and quick transfer of oxygen species and intermediates are generally considered as the main factors for ceria to promote the oxygen-involving reactions (not only for OER but also for ORR), and characterizations of those properties are necessary to unveil the relationship between oxygen adsorption/desorption ability and catalytic property for those ceria- and Ce-incorporated electrocatalysts, which were seldom reported. Recently, measuring the specific surface areas of various electrocatalysts under different atmospheres of oxygen and nitrogen based on the Brunauer–Emmett–Teller method was proposed by Feng et al. [43]. Under N_2 atmospheres, the specific surface areas of FeOOH and $FeOOH/CeO_2$ were almost the same, whereas $FeOOH/CeO_2$ exhibited a much larger specific surface area under oxygen atmosphere than FeOOH, demonstrating the high oxygen storage capacity caused by ceria. Another approach of the oxygen temperature-programmed desorption (O_2-TPD) method was adopted by our group to directly evaluate the oxygen adsorption capacity of various electrocatalysts [49]. For instance, the oxygen adsorption capacity for pure NiO is only 15.5 μmol g^{-1}, whereas that of ceria-embedded NiO is 47.4 μmol g^{-1}, apparently suggesting the promotion in adsorbing oxygen-containing species and intermediates for NiO after incorporating with ceria.

The comparisons in catalytic propertabove electrocatalsyts and their counterparts with RE element-incorporations for OER are listed in Table 2. Thus, from the aforementioned literature, it can be learned that Ce is the most adopted RE element to modify other transition metal–based electrocatalysts by doping Ce ions and introducing ceria. Generally, several factors for Ce-based species are responsible for the enhanced OER activity and durability: (1) the strong interactions between host materials and ceria (as well as Ce ions by doping) to modulate the electronic structures of electrocatalysts, (2) the oxygen buffer property to accelerate the adsorption, desorption, and transfer of oxygen species and intermediates, (3) more defects and vacancies caused by Ce for hosts as catalytically active sites, and (4) the prevention of hosts from corrosion and dissolution to preserve the stability. Of note, because ORR somehow is a 'reverse' reaction for OER, benefits of ceria for OER are also generally applicable for ORR, which will be discussed in details in the following section.

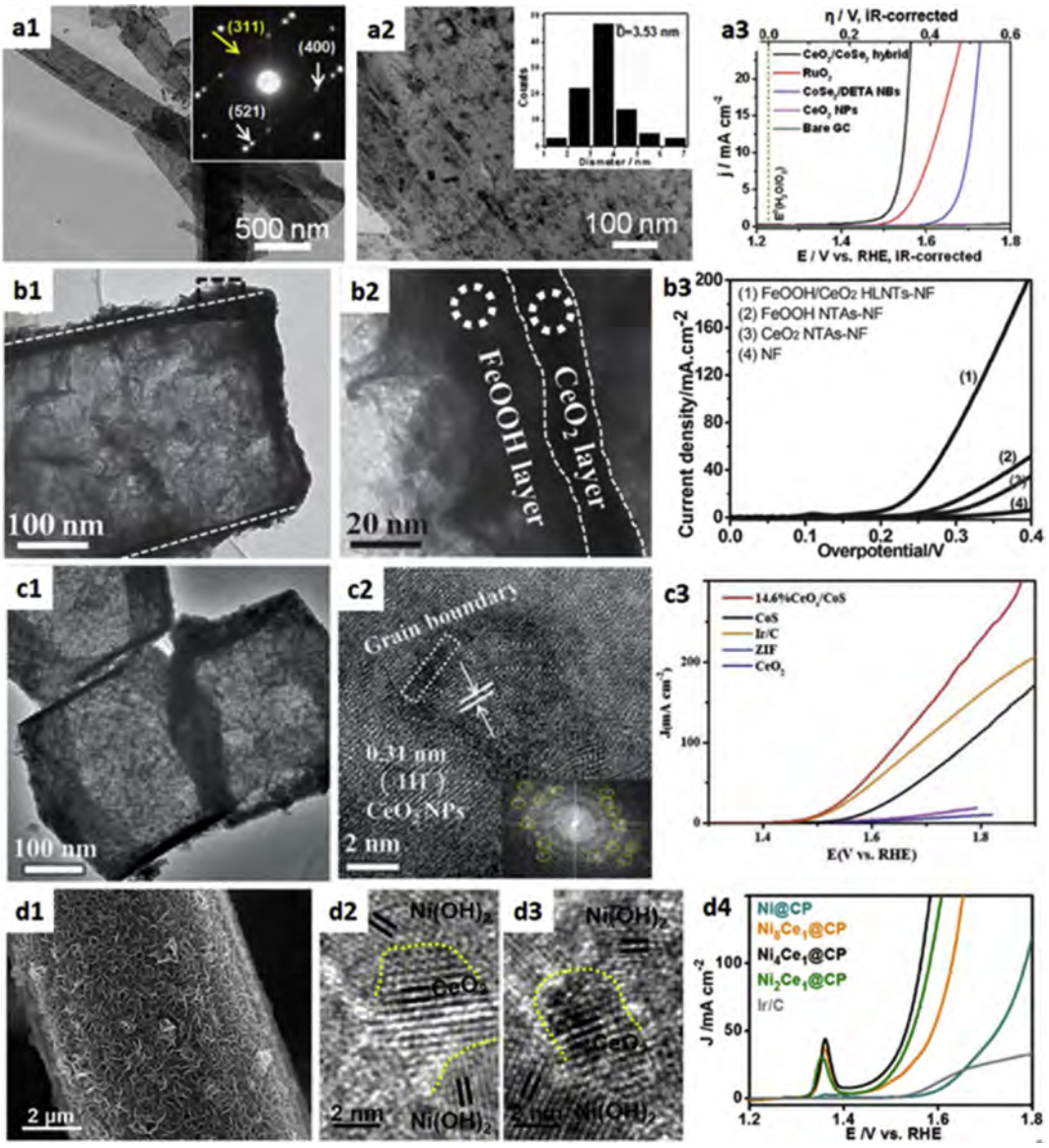

Fig. 6. (a1, a2) TEM images with different magnifications of $CeO_2/CoSe_2$ nanobelt composite prepared at 278 °C for 1 h. The inset in (a1) shows the corresponding SAED pattern, and the inset in (a2) shows the corresponding particle size histogram. (a3) Polarization curves with iR correction for OER on bare GCE and modified GCEs comprising the $CeO_2/CoSe_2$ nanobelt composite, RuO_2, $CoSe_2$/DETA NBs, and CeO_2. Reproduced with permission from Ref. [42]. Copyright 2015, WILEY-VCH. (b1) TEM image of a typical CeO_2/FeOOH HLNT. (b2) TEM image of FeOOH/CeO_2 HLNT in the rectangle. (b3) Polarization curves of FeOOH/CeO_2 HLNTs-NF, FeOOH NTAs-NF, CeO_2 NTAs-NF, and NF at the scan rate of 5 mV s^{-1}. Reproduced with permission from Ref. [43]. Copyright 2016, WILEY-VCH. (c1) TEM images for 14.6% CeO_x/CoS. (c2) The HRTEM images and corresponding SAED pattern (the inset) of 14.6% CeO_x/CoS. (c3) LSV curves of 14.6% CeO_x/CoS, CoS, CeO_2, ZIF-67, and Ir/C catalysts for the OER. Reproduced with permission from Ref. [48]. Copyright 2016, WILEY-VCH. (d1) SEM image of Ni_4Ce_1@CP. (d2, d3) Enlarged HRTEM images of Ni_4Ce_1@CP. (d4) OER polarization curves of Ni@CP, Ni_8Ce_1@CP, Ni_4Ce_1@CP, Ni_2Ce_1@CP, and commercial Ir/C. Reproduced with permission from Ref. [50]. Copyright 2018, American Chemical Society. OER, oxygen evolution reactionTEM, transmission electron microscopy; SAED, selected area electron diffraction; GCE, glassy carbon electrode; HLNT, heterolayered nanotubes; DETA, diethylenetriamine; NBs, nanobelts; NF, Ni foam; NTAs, nanotube arrays; LSV, linear sweep voltammetry; HRTEM, high-resolution transmission electron microscopy; CP, carbon paper; RHE, reversible hydrogen electrode.

5. RE element–incorporated electrocatalysts for ORR

ORR is an important cathodic half reaction with a two-electron or four-electron process for both polymer electrolyte membrane fuel cells and rechargeable metal–air batteries, but its slow kinetics limited the power output. Pt has been considered as the most active ORR electrocatalyst for a very long time, but the disadvantages such as high price and durability are promoting the modification of Pt-based electrocatalysts and development of novel non-precious transition metal–based electrocatalysts as alternatives. Lately, research has demonstrated the improvement in activity for various electrocatalysts by incorporating with RE elements to regulate their structural and catalytic properties, and two strategies of alloying with electrocatalysts and decorating ceria onto electrocatalysts are widely reported.

5.1. Alloying Pt with different RE elements for ORR

Recently, a series of research carried out by Chorkendorff et al contributed much to investigate the influences of RE elements on the structural and catalytic properties of Pt-based alloy electrocatalysts for ORR [53–56]. Following the Sabatier principle, the descriptor of ΔE_{OH} binding energy controls the ORR activity for various metals to obtain a volcano-type curve, where a ΔE_{OH} ~0.1 eV weaker than Pt (111) yields the optimum value. At first, the electrocatalysts of Pt alloyed with Sc and Y, Pt_3Sc and Pt_3Y, were proposed as active and stable polycrystalline materials for ORR, matching the volcano curve well with respect to the theoretically derived ΔE_O. The positive shift of ~20 mV in half-wave potential for Pt_3Sc, compared with Pt, and ~60 mV for Pt_3Y demonstrated the

Table 2
Summary of the OER catalytic property of various electrocatalysts before and after RE element incorporation.

Electrocatalysts	Overpotential @ 10 mA cm^{-2} (mV)	Tafel slope (mV dec^{-1})	Electrolyte	Ref.
NiO_x-Au	>380	–	1 M NaOH	[39]
$NiCeO_x$-Au	271	–		
NiFe-LDH/CNT	299	92	1 M KOH	[40]
5% Ce-NiFe-LDH/CNT	227	33		
$CoSe_2$	288	44	0.1 M KOH	[42]
$CeO_2/CoSe_2$	~470	66		
FeOOH NTAs-NF	250 (@ 9.86 mA cm^{-2})	113.7	1 M NaOH	[43]
FeOOH/CeO_2 HLNTs-NF	250 (@ 31.3 mA cm^{-2})	92.3		
PIZA-1-400	430	53	1 M KOH	[44]
CeO_2@PIZA-1-400	370	47.6		
$Ni(OH)_2$/NOSCF	270 (at onset potential)	57	1 M KOH	[45]
$CeO_2/Ni(OH)_2$/NOSCF	240 (at onset potential)	65		
Fe–Ni	370	49	0.1 M KOH	[46]
Hematite-modified Ce–Ni	340	45		
CoO_x	331	70	1 M NaOH	[47]
CeO_x/CoO_x	313	66		
CoS	347	81	1 M KOH	[48]
14.6% CeO_x/CoS	269	50		
NiO	467	140.7	1 M KOH	[49]
Ce–NiO-E	382	118.7		
$Ni(OH)_2$@CC	>380	83.3	1 M KOH	[50]
$Ni(OH)_2$–CeO_2@CC	220	81.9		

CNT, carbon nanotube; OER, oxygen evolution reaction; LDH, layered double hydroxide; RE, rare earth; PIZA-1, porphyrinic Illinois zeolite analogue no. 1; NTAs, nanotube arrays; NF, Ni foam; HLNTs, heterolayered nanotubes; NOSCF, N, O, S doped carbon foam; CC, carbon cloth.

excellent activity of these Pt-based bulk alloys in acid with optimized ΔE_O [53]. Later, to provide insight into the origin of the enhanced activity of Pt–Y alloy, Pt_xY nanoparticles with various sizes were prepared by gas aggregation [14]. The ORR activity increased with increase in the size of Pt_xY alloy nanoparticles; meanwhile, there was an increase in compressive strain and a decrease in average nearest neighbor Pt-–Pt distance, suggesting that the specific activity was a function of the strain. Furthermore, for Pt_xY alloy nanoparticles, both the specific activity and strain decreased after stability tests, whereas Pt-–Pt distance increased. Dealloying *via* diffusion of Y atoms into the bulk and the formed overlayer of Pt shell with thickness of several atoms during ORR process is believed to hinder the strong interaction between Pt and Y, which decreased the strain, increased the Pt-–Pt distance, and resulted in the deteriorated activity [14]. Similar relationship between the compressive strain (as well as Pt-–Pt distance) and specific activity for ORR was also established for Pt_xGd electrocatalysts, and the decrease in remarkable activity was also ascribed to the formation of Pt outlayer shell [54]. Further investigation on the strain and crystallinity of the Pt overlayer was carried out with a combination of experimental measurement and DFT calculations on Y/Pt (111) and Gd/Pt (111), the electrochemically formed Pt overlayer was proposed to be responsible for the reduced compressive strain and ORR activity [55]. Lately, thorough investigation of the periodic changes in radius of lanthanides with increase in filling of the 4f shell on the ORR activity and stability provided a good pathway to engineer the compression strain, where RE elements, including La, Ce, Sm, Gd, Tb, Dy, and Tm, and alkaline earth elements such as Ca are used [56]. The thickness of electrochemically formed Pt overlayer (Fig. 7a), lattice parameter, catalytic activity, and compressive strain were closely dependent on the radius of foreign RE elements. The results exhibited the dependence of activity loss and dissolution potential of RE elements were the functions of lattice parameter and strain (Fig. 7b), demonstrating that strain was another descriptor of stability. In other words, a proper strain could not only improve the activity of Pt with optimal lattice parameter but also induce the destabilization of the Pt overlayer to facilitate the surface mobility of residual RE elements for dissolution. Thus, the lattice parameter of Pt alloys also followed a Sabatier volcano (Fig. 7c): alloys on the left bind OH too weakly, whereas those on the right bind OH too strongly. On the other hand, beyond a certain level of bulk strain, the overlayer could be unstable, causing the Pt-–Pt parameter of the overlayer and activity of alloy to relax toward a much lower level of surface strain. Therefore, this work suggested the strain effect could only weaken the binding of H and OH to a certain level and either larger or smaller strain would not contribute to the activity and stability most.

5.2. Noble metals promoted by CeO_2 for ORR

Besides fabricating Pt alloys with RE elements, preparing composites with CeO_2 as the additive and promotor is also a novel developed method to improve the catalytic activity and stability for ORR in both acidic and alkaline solutions and decrease the mass of noble metals such as Pt and its alloys PtAu and Pt_3Pd_1 as the active electrocatalysts [57–62]. For ceria, its advantages for enhancing OER are also applicable to promote the activity of other electrocatalysts for ORR. For instance, by adding CeO_2 and treating under nitrogen atmosphere to regulate the surface condition of PtAu alloy nanoparticles, the Au core/Pt shell–structured alloys were tightly loaded on ceria supports with strong interaction, as demonstrated by Liu et al. [57]. With higher annealing temperatures, the surface Pt-richer state for PtAu alloys and the stronger interaction between alloys and ceria would facilitate the ORR process, which was later proved by the enhanced catalytic activity with positive shift in half-wave potentials. Moreover, Luo et al. [58] demonstrated the Pt/CeO_x/C electrocatalysts from a Ce-based MOF structure as an efficient electrocatalyst for ORR and H_2/O_2 microlaminar flow fuel cell. The result showed that the interaction between Pt nanoparticles and Ce-based MOF-derived CeO_x stabilized Pt^0 and Ce^{3+} species, as well as the modified surface with higher Pt active surface area promoted the H and CO adsorption, leading to the higher activity and durability for ORR than commercial Pt/C. Similar results were also observed for the case of Pt_3Pd_1/CeO_2/C [59], Pt/CeO_2/C [60], Pt/CeO_x/C [61], and Pt/CeO_2/multi-wall carbon nanotubes (MWCNTs) [62] to prevent the activity from great loss because of the good interaction between noble metals and CeO_2 to stabilize noble metal nanoparticles. For example, Masuda et al. [61] used the *in situ* X-ray adsorption fine structure that revealed the inhibition of Pt oxidation by the oxidation of Ce^{3+} into Ce^{4+} in CeO_x instead of Pt that led to the higher activity. Li et al. [62] characterized the electrocatalysts of Pt/C and Pt/CeO_2/MWCNTs after aging test and revealed the good preservation of Pt nanoparticle size and activity without significant change and loss (Fig. 8) for the electrocatalyst with ceria, ascribing to the strong interaction between Ce^{3+} and oxygen vacancy–rich ceria and Pt nanoparticles to prevent Pt from aggregation.

5.3. Non-precious metal–based electrocatalysts promoted by CeO_2 for ORR

Recently, the promotion in activity by ceria for non-precious transition metal–based electrocatalysts for ORR has also been reported [63–66]. For instance, the oxygen buffer property of ceria originated from the fast Ce^{3+}/Ce^{4+} redox transfer and the oxygen storage property of ceria promoted the supply and convert of oxygen intermediates, as depicted by Liu et al. [63] in the Co_3O_4–CeO_2/C electrocatalyst. Furthermore, this electrocatalyst also exhibited a higher discharge voltage plateau when used as the cathode in Al–air batteries, suggesting the efficient promotion from ceria to boost ORR process of Co_3O_4. Moreover, Xia et al. [65]

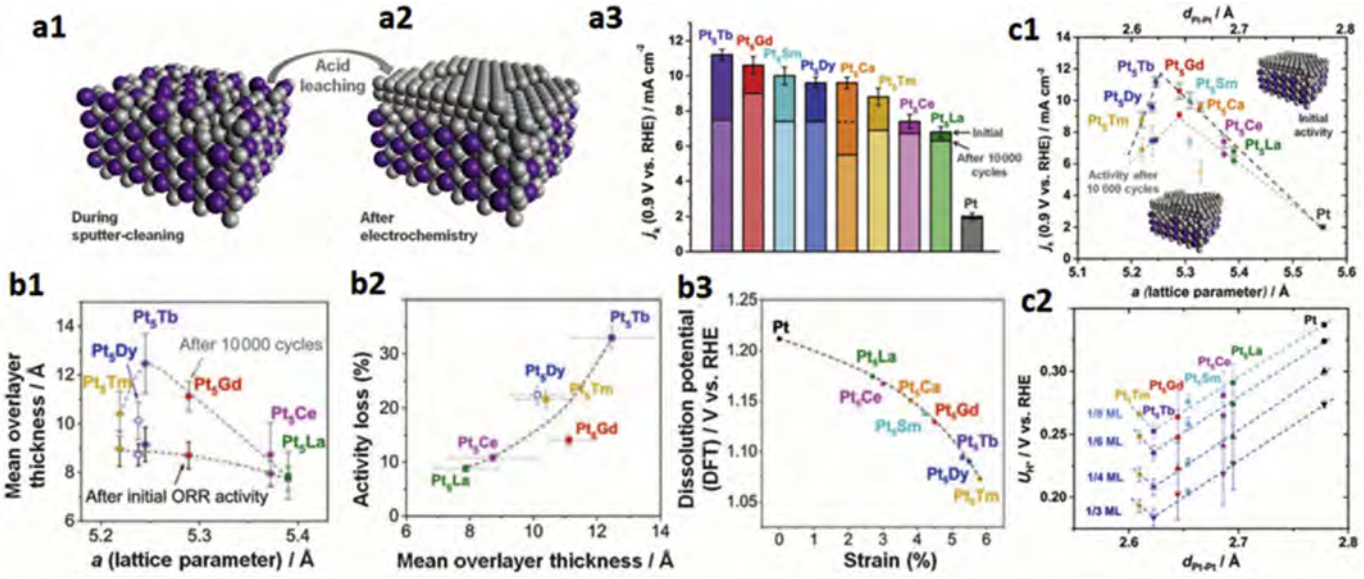

Fig. 7. (a) Schematic views and electrochemical properties of polycrystalline Pt_5M (M = lanthanide or alkaline earth metal) electrocatalysts. The three-dimensional view of the Pt_5M structure (a1) during sputter cleaning and (a2) after electrochemistry. (a3) Kinetic current density, j_k, of Pt_5M and Pt before and after stability test. (b) Pt overlayer thickness as a function of the lattice parameter and activity loss. (b1) Estimated average thicknesses of the Pt overlayer for Pt_5Tm, Pt_5Dy, Pt_5Tb, Pt_5Gd, Pt_5Ce, and Pt_5La after initial ORR activity and after stability test, as a function of *a* lattice parameter. (b2) Percentage of activity loss after stability test as a function of the Pt overlayer thickness. (b3) Slab stability represented as dissolution potential versus the strain of the Pt overlayer on Pt_5M. (c) Experimental volcano-type relationships between activity, H adsorption, and Pt-–Pt distance. (c1) Kinetic current density at 0.9 V on polycrystalline Pt_5M electrocatalysts versus the lattice parameter *a* of bulk Pt_5M (lower axis) and bulk $d_{Pt\text{-}Pt}$ (upper axis). (c2) Relation between the potential necessary to adsorb 1/8, 1/6, 1/4, and 1/3 monolayers (MLs) of H (U_H) from the cyclic voltammograms (CVs) in the H adsorption and d_{Pt-Pt}. Reproduced with permission from Ref. [56]. Copyright 2016, American Association for the Advancement of Science. ORR, oxygen reduction reaction; RHE, reversible hydrogen electrode.

showed the enhanced ORR activity of Co, N-doped carbon nanosheets by decorating small ceria nanoparticles. The oxygen buffer property of ceria was verified by the O_2-TPD method to prove the enhanced oxygen adsorption capacity and synergistic effect between them.

5.4. Ce-based electrocatalysts for ORR

Lately, except collaborating with other transition metal–based electrocatalysts, Ce-based composites are also investigated as electrocatalysts for ORR. Several typical samples of carbon-encapsulated defect-rich CeO_{2-x}, Ce_2O_2S on N, S dual-doped carbon, CeO_2/reduced graphene oxide, and $CeO_2/CePO_4$ with N,P-codoped carbon shells are reported as catalytically active materials for ORR [67–70]. However, the catalytic activity of the aforementioned Ce-based electrocatalysts is still not satisfactory, compared with that of Co– and Fe-based materials. Moreover, the catalytic mechanism of Ce-based samples is not very clear. Although Ce^{3+} is considered to modulate the binding energy to absorb oxygen species during the adsorption, dissociation, and reduction of oxygen molecules [68], more experimental and theoretical evidence is still lacking and required to explain.

Overall, the combination of RE elements, oxides, and other RE element–based (especially Ce-based) materials can significantly facilitate the ORR property of host electrocatalysts in both acidic and basic electrolytes (see Table 3 for above mentioned electrocatalysts). For Pt-based alloys, optimization in crystalline strain and lattice parameter contributes to the enhanced catalytic activity. For the significant promotor of ceria, its positive effects described for OER on oxygen species are also feasible for the ORR process. More importantly, the strong interaction between noble metals and ceria can stabilize nanosized noble metals to prevent them from aggregation and modulate their structural and electronic features with larger active surface areas for catalysis.

6. RE element–incorporated electrocatalysts for MOR

Direct methanol fuel cells (DMFCs) have been considered to be a promising power source to portable devices and electrical vehicles because of their high volumetric energy density, abundant sources of methanol, and environmentally friendly effect. The collaboration of noble metals such as Pt with RE elements is also attracting increasing attention with the purposes to decrease the usage of noble metals, ameliorate the antipoison ability of catalysts, and stabilize noble metals to further improve the catalytic activity and stability for the MOR process. CeO_2 has been broadly used as an efficient oxide to promote the catalytic activity of Pt and its alloy for MOR because of its high oxygen storage capacity, good mechanical resistance, and anticorrosion ability in acidic and alkaline media over the past decades [59,71–83]. Typically, Xu et al. [82] demonstrated the excellent catalytic activity and durability of Pt/CeO_2/polyaniline (PANI)-arrayed structure for MOR, compared with that of commercial Pt/C. This enhancement is ascribed to the following reasons: the hollow array structure to facilitate the transportation

Table 3
Summary of the ORR catalytic property of various electrocatalysts before and after RE element incorporation.

Electrocatalysts	Onset potential (OP) or half potential (HP) (V)	Tafel slope (mV dec^{-1})	Electrolyte	Ref.
Pt/C	0.8 (OP)	N/A	0.1 M $HClO_4$	[59]
Pt_3Pd_1–CeO_2/C	0.91 (OP)	N/A		
Pt/C	0.85 (HP)	N/A	0.1 M $HClO_4$	[60]
Pt/10CeO_2/C	0.86 (HP)	N/A		
Co_3O_4/KB	0.73 (HP)	N/A	0.1 M KOH	[63]
Co_3O_4–CeO_2/KB	0.83 (HP)	83.9		
HPCNs	0.882 (OP), 0.799 (HP)	101	0.1 M KOH	[65]
Ce-HPCNs	0.923 (OP), 0.831 (HP)	91		

ORR, oxygen reduction reaction; RE, rare earth; KB, ketjenblack; HPCNs, hierarchical porous carbon nanosheets.

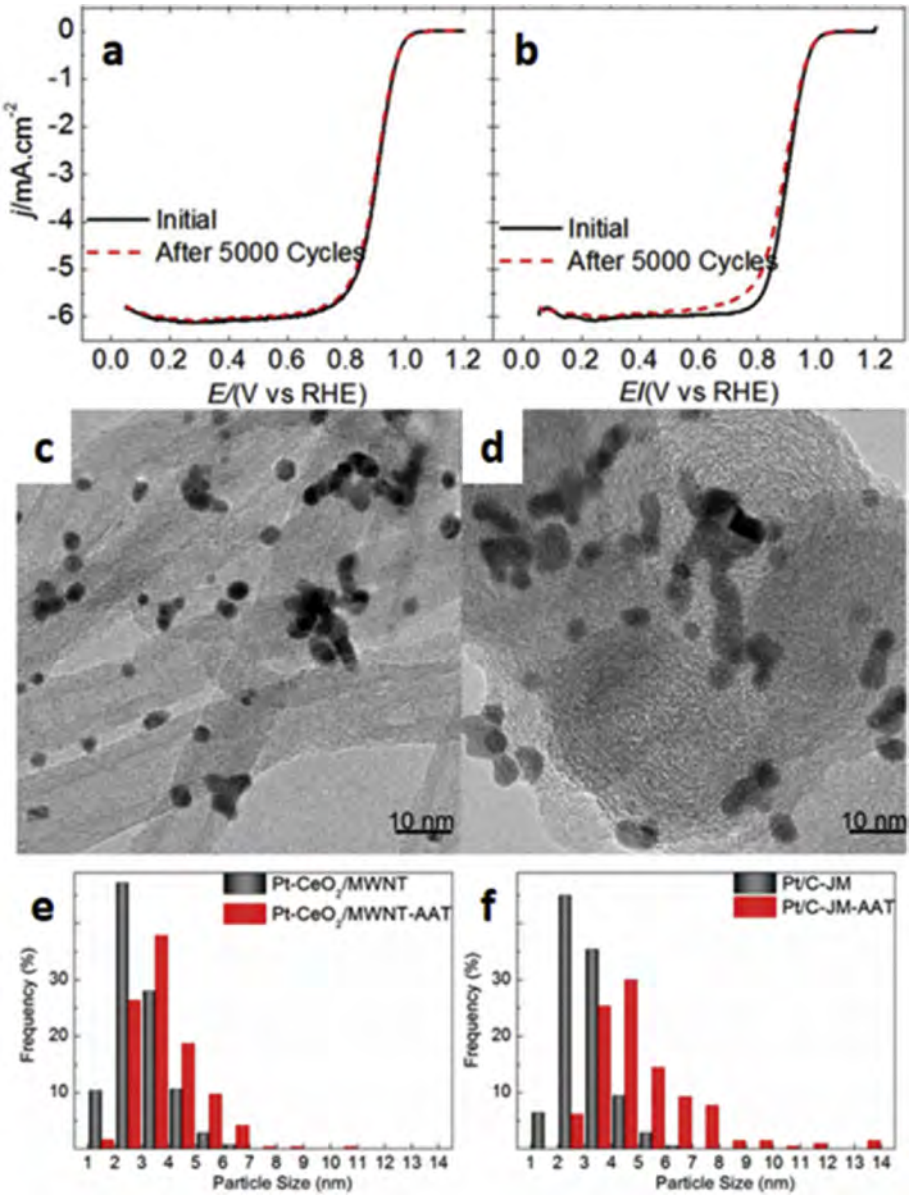

Fig. 8. ORR polarization curves, TEM images, and particle diameter distribution of (a, c, e) Pt–CeO_2/MWNT and (b, d, f) Pt/C-JM after accelerated aging test. Reproduced with permission from Ref. [62]. Copyright 2018, WILEY-VCH. ORR, oxygen reduction reaction; TEM, transmission electron microscopy; MWNT, multi-wall nanotube.

of electrons and active species; the electron delocalization among PANI π—conjugated ligands, Ce 3d orbitals, and Pt 4f orbitals to alter the electronic structure and d-band center of Pt; and the promotion in Pt dispersion caused by ceria. Besides the aforementioned benefits, the other two advantages from ceria are also related to the enhanced activity. On the one hand, the triple-phase interfacial region between ceria, Pt, and the atmosphere/solution also played a very important role to improve the activity. The charge transfer between Pt and Ce^{4+} can lead to the trapping and embedding of $Pt^{\delta+}$ species into ceria to stabilize Pt nanoparticles and formation of more vacancies. Moreover, the change in the microstructure of ceria and transfer of activated ions to the surface of Pt can be contributed to this triple phase to enhance this activity [76,83]. On the other hand, the carbonaceous species as the intermediates of linearly bonded C=O strongly absorb onto the Pt surface (Pt–C=O or Pt-CO_{ads}) to block the active Pt surface and hinder the reaction during anodic methanol oxidation. Ceria is known as an excellent catalyst to catalyze the oxidation of CO; thus, the existence of ceria can improve the antipoison property and CO tolerance of Pt by catalyzing the OH group at the triple-phase interface to react with absorbed CO species on Pt particles *via* the bifunctional mechanism [71,72,74,80]. This mechanism is represented by the following equations 1-3:

$$CeO_2 + H_2O \rightarrow CeO_2\text{-}OH_{ads} + H^+ + e^- \quad (1)$$

$$CeO_2\text{-}OH_{ads} + Pt\text{-}CO_{ads} \rightarrow CeO_2 + Pt + CO_2 + H^+ + e^- \quad (2)$$

and/or

$$Pt\text{-}CeO_2 + xCO \rightarrow Pt\text{–}CeO_{2\text{-}x} + xCO_2 \quad (3)$$

Therefore, the introduction of ceria into electrocatalysts for MOR is an efficient approach to modulate the crystalline and electronic structures of active sites and prevent the noble metals from CO poisoning to improve the durability. Moreover, the noble

metal free–catalyst of nanosized CeO_2 was recently reported to be highly active for MOR by Kaur et al. [84]. Specifically, the electrocatalysts of ceria-decorated nanocrystalline zeolite (Nano-ZSM-5) on glassy carbon electrode exhibited remarkable activity and stability (Fig. 9a and b) and CO tolerance for MOR compared with commercial 20% Pt/C. Brønsted acidic sites of Nano-ZSM-5 enable the adsorption of OH^- from the electrolyte and its reaction with ceria to form $Ce(OH)_x$ (Fig. 10c). With a low energy, the $Ce(OH)_x$ species can reversibly release OH^- and regenerate CeO_2, as given in equation (4).

$$[CeO_2/\text{Nano-ZSM-5}] + OH^- + H_2O \leftrightarrow [Ce(OH)_x/\text{Nano-ZSM-5}] + e^- \quad (4)$$

Then, methanol is absorbed by the Brønsted acidic sites of Nano-ZSM-5, and its electrooxidation is catalyzed by the as-formed $Ce(OH)_x$ species to accelerate the dehydrogenation of absorbed $-CH_3OH_{ads}$ species *via* a stepwise process, finished by the release of CO_2. The proposed mechanism is listed in the equations 5-11.

$$[Ce(OH)_x/\text{Nano-ZSM-5}] + CH_3OH \rightarrow [Ce(OH)_x/\text{Nano-ZSM-5}](CH_3OH)_{ad} \quad (5)$$

$$[Ce(OH)_x/\text{Nano-ZSM-5}](CH_3OH)_{ad} + OH^- \rightarrow [Ce(OH)_x/\text{Nano-ZSM-5}](CH_2OH)_{ad} + H_2O + e^- \quad (6)$$

$$[Ce(OH)_x/\text{Nano-ZSM-5}](CH_2OH)_{ad} + OH^- \rightarrow [Ce(OH)_x/\text{Nano-ZSM-5}](CHOH)_{ad} + H_2O + e^- \quad (7)$$

$$[Ce(OH)_x/\text{Nano-ZSM-5}](CHOH)_{ad} + OH^- \rightarrow [Ce(OH)_x/\text{Nano-ZSM-5}](COH)_{ad} + H_2O + e^- \quad (8)$$

$$[Ce(OH)_x/\text{Nano-ZSM-5}](COH)_{ad} + OH^- \rightarrow [Ce(OH)_x/\text{Nano-ZSM-5}](CO)_{ad} + H_2O + e^- \quad (9)$$

$$[Ce(OH)_x/\text{Nano-ZSM-5}](CO)_{ad} + OH^- \rightarrow [Ce(OH)_x/\text{Nano-ZSM-5}](COOH)_{ad} + e^- \quad (10)$$

$$[Ce(OH)_x/\text{Nano-ZSM-5}](COOH)_{ad} + OH^- \rightarrow [Ce(OH)_x/\text{Nano-ZSM-5}] + CO_2 + H_2O + e^- \quad (11)$$

Because of the synergistic contribution given by nanosized CeO_2 and Nano-ZSM-5, this noble metal–free electrocatalyst presented high activity for MOR and durability in alkaline media, and this provides a novel and low-cost pathway for the development of DMFCs. The catalytic performances of electrocatalsyts with and without RE element–incorporation are summarized in Table 4 to have a better view on the improvement from RE elements.

7. RE element–incorporated electrocatalysts for other electrochemical reactions

Ceria with the reverse Ce^{3+}/Ce^{4+} redox pair and oxygen storage ability is of special interest and importance for catalysis among various RE element oxides and is being broadly used in electrocatalysis. Except for the application of various RE elements in HER, OER, ORR, and MOR, other electrochemical reactions are also recently promoted by RE elements, including the electrochemical oxidation of ethanol [85–88], formic acid [89], hydrazine [90], ammonia [91], and so on, as well as the electrochemical CO_2 reduction reaction [92,93] and N_2 fixation to synthesize NH_3 [94,95].

Typically, the mechanism of electrochemical ethanol oxidation is similar to that of electrocatalytic methanol oxidation, and Xu and Shen [85,86] demonstrated the promotion in activity of the Pt/C catalyst by incorporating with ceria. By benefiting the formation of oxygen-containing species with lower potentials to transform CO-like species on Pt to ceria, the $Pt/CeO_2/C$ catalysts exhibited better activity and durability for ethanol oxidation [86].

Electrochemical CO_2 reduction reaction is attracting increasing attention to realize the efficient conversion of CO_2 to other chemicals. Ceria is recently used as the promotor of catalytically active metals for CO_2 reduction. For example, by building the Au-CeO_x heterogeneous structure (Fig. 10a), the activity and selectivity of electrochemical CO_2 reduction reaction is significantly enhanced (Fig. 10b and c), as demonstrated by Gao et al. [92]. The experimental results showed the enhanced CO_2 adsorption and activation by the Au-CeO_x interface to promote the activation of CO_2 at the interface sites and facilitate the subsequent adsorption of CO_2 on ceria terraces. Moreover, the facile dissociation of water at interfacial Ce^{3+} sites promotes the formation of surface hydroxyl groups, which can help reduce CeO_x species and stabilize $CO_2^{\delta-}$ species. The

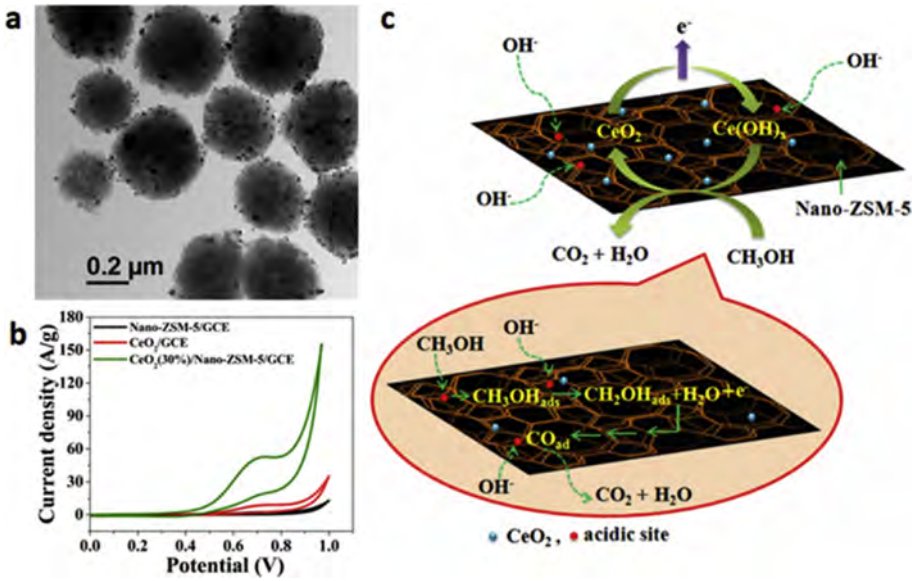

Fig. 9. (a) TEM images of CeO_2 (30%)/Nano-ZSM-5. (b) Comparison of CVs at CeO_2 (30%)/Nano-ZSM-5/GCE, CeO_2/GCE, and Nano-ZSM-5/GCE in the presence of 0.5 M methanol in 0.5 M NaOH solution at a scan rate of 50 mV/s. (c) Schematic representation for the electrochemical oxidation of methanol at CeO_2 (30%)/Nano-ZSM-5/GCE. Reproduced with permission from Ref. [84]. Copyright 2016, American Chemical Society. CVs, cyclic voltammograms; TEM, transmission electron microscopy; GCE, glassy carbon electrode.

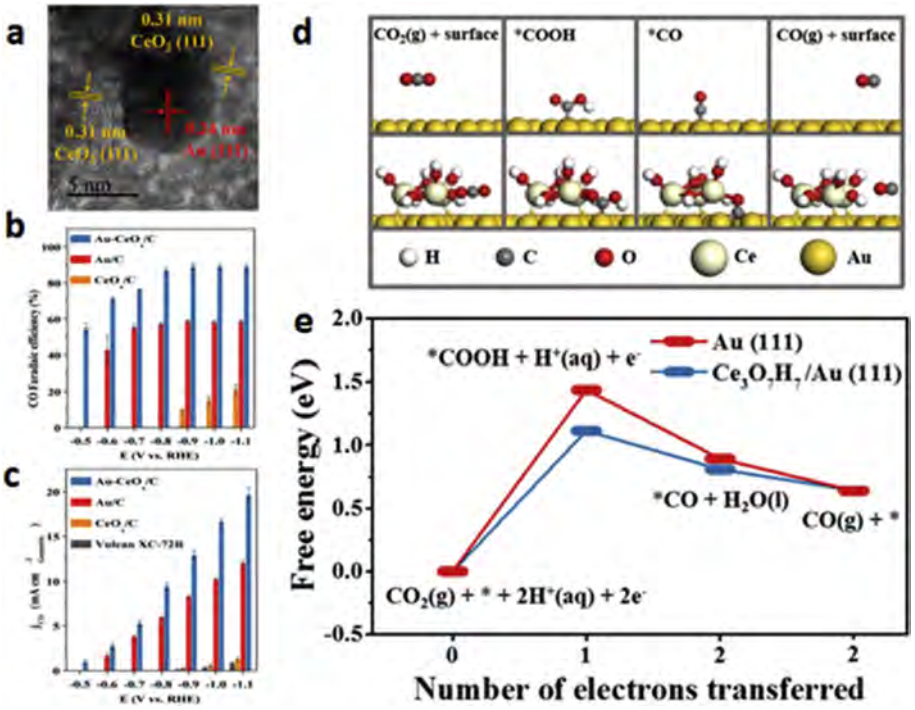

Fig. 10. (a) HRTEM image of the Au-CeO_x/C catalyst. (b) Faradaic efficiency and (c) geometric partial current density for CO production over Au/C, CeO_x/C, and Au-CeO_x/C catalysts in CO_2-saturated 0.1 M $KHCO_3$ solution and their dependence on the applied potentials. DFT calculations of CO_2RR at 0 V vs RHE on Au (111) and $Ce_3O_7H_7$/Au (111) surfaces. (d) Optimized structures for the main intermediates. (e) Calculated free energy diagram. '*' indicates an adsorbed surface species. Reproduced with permission from Ref. [92]. Copyright 2017, American Chemical Society. DFT, density functional theory; HRTEM, high-resolution transmission electron microscopy; RHE, reversible hydrogen electrode.

DFT calculations revealed the lower free energy for the formation of carboxyl species (*COOH), which was the potential limiting step, at the CeO_x/Au (111) interface than on Au (111) (Fig. 10d and e). Therefore, the metal–oxide interface of Au-CeO_x and special property of CeO_x contributed greatly to the enhanced activity for CO_2 reduction. Moreover, single atomic Cu substitution in CeO_2 was theoretically predicted to enrich multiple oxygen vacancies around Cu atoms and would be highly effective for the electroreduction of a single CO_2 molecule to CH_4, as exhibited by Wang et al. [93]. Their further experimental investigation proved the high activity and faradaic efficiency of Cu–CeO_2, resulting from the atomic dispersion of Cu and oxygen vacancies from the CeO_2 framework.

Electrochemical fixation of N_2 into NH_3 is a green approach to produce NH_3 without carbon dioxide emission and large energy waste. Lately, Lv et al. [94] demonstrated the hybrid nanofibers of $Bi_4V_2O_{11}/CeO_2$ with amorphous structure, which was induced by CeO_2. This $Bi_4V_2O_{11}/CeO_2$ hybrid electrocatalyst presented outstanding activity and yield for NH_3 production because the participation of CeO_2 facilitated to establish the band alignment in the proposed catalyst, induce advantageous features of abundant active sites, and promote interfacial charge transfer. Moreover, a nanosheet-structured Y_2O_3 was proposed by Li et al. [95] to be the electrocatalyst for N_2 fixation under ambient conditions. Both experimental and theoretical investigations explained the good

Table 4
Summary of the MOR catalytic property of various electrocatalysts before and after RE element incorporation.

Electrocatalysts	Peak current density	Onset potential (mV)	Electrolyte	Ref.
Pt-O CNT	383 mA mg^{-1}Pt	N/A	1 M $HClO_4$ + 1 M CH_3OH	[71]
Pt-CPO CNT	638 mA mg^{-1}Pt	N/A		
Pt/C	443 mA mg^{-1}Pt	0.52	0.5 M H_2SO_4 + 1 M CH_3OH	[73]
Pt–CeO_2/C-RME	647 mA mg^{-1}Pt	0.46		
Pt/CNTs	1.6 mA mg^{-1}Pt	0.43	1 M H_2SO_4 + 1 M CH_3OH	[74]
Pt–CeO_2/CNTs	10.3 mA mg^{-1}Pt	0.35		
30 PtRu	2.8 mA cm^{-2}Pt	N/A	0.5 M H_2SO_4 + 0.5 M CH_3OH	[76]
30Pt–CeO_2/C	1.63 mA cm^{-2}Pt	N/A		
Pt/rGO	66.8 mA mg^{-1}Pt	N/A	0.5 M H_2SO_4 + 0.5 M CH_3OH	[79]
CeO_2/rGO/Pt	194.5 mA mg^{-1}Pt	N/A		
Pt/C	9.4 mA cm^{-2}	N/A	0.5 M H_2SO_4 + 1 M CH_3OH	[80]
Pt/CeO_2-HP/C	14.6 mA cm^{-2}	N/A		
Pt/C	185.8 mA mg^{-1}Pt	N/A	0.5 M H_2SO_4 + 1 M CH_3OH	[81]
Pt–7% CeO_2/C	440.1 mA mg^{-1}Pt	N/A		
Pt/PANI HNRAs	225.8 mA mg^{-1}Pt	N/A	0.5 M H_2SO_4 + 0.5 M CH_3OH	[82]
Pt/CeO_2/PANI HNRAs	361.33 mA mg^{-1}Pt	N/A		
CeO_2	9.1 mA mg^{-1}	>0.55	0.5 M NaOH + 0.5 M CH_3OH	[84]
CeO_2 (30%)/Nano-ZSM-5	52.6 mA mg^{-1}	<0.45		

CNT, carbon nanotube; MOR, methanol oxidation reaction; PANI, polyaniline; RE, rare earth; HNRAs, hollow nanorod arrays; CPO CNT, CeO_2 deposited PO-CNTs; rGO, reduced graphene oxide; RME, reverse microemulsion.

catalytic activity and stability of Y_2O_3, making it a promising electrocatalyst to fix N_2. Thus, the introduction of not only ceria but also other RE element–based compounds is rising lately to promote the catalytic activity and selectivity of host materials for various electrocatalytic reactions.

8. Summary and perspectives

8.1. Summary

In this present review, we summarized the recent developments of RE element–incorporated electrocatalysts and their applications in various electrocatalytic reactions, such as HER, OER, ORR, MOR, and so on. Generally, there are three approaches to realize the collaboration of RE elements with other transition metals, namely, alloying with other metals, doping RE element ions into transition metal–based electrocatalysts, and introducing RE element–based compounds (such as oxides) into hosts. Among various RE element oxides, ceria attracted great interest in the application of electrocatalysis because of its special structural properties with Ce^{3+}/Ce^{4+} redox pair, abundant vacancies, high oxygen storage capacity, and good chemical and mechanical stability to promote those oxygen-involving reactions. The literature published over the past decades has clearly demonstrated the effectiveness of incorporating with RE elements to modulate the electronic and crystalline structures, tune the interactions between catalytically active species and substrates, and regulate the surface properties of electrocatalysts, which subsequently improve the catalytic activity and durability of host electrocatalysts and reduce the amount of noble metals used. Therefore, incorporating with RE elements would lead to a novel path to further modify the catalytic property of various heterogeneous electrocatalysts to boost their catalytic properties for different electrochemical reactions.

8.2. Perspectives

Although great improvements have been realized, understanding the roles and effects of RE elements in electrocatalysis is still far from being solved. To have further insight, there are still many critical issues for RE element–incorporated electrocatalysts and electrocatalytic processes to be addressed.

(1) Rational synthesis of RE element–incorporated electrocatalysts with proper amounts of RE elements. Generally, to optimize the amount of RE elements used during the preparation of electrocatalysts, RE element sources with large ranges and intervals in amount are adopted, in which these large variations in RE elements may not provide the accurate control to the corresponding synthesis. Recently, Haber et al. [96,97] investigated the optimal composition and structural property of a (Ni-Fe-Co-Ce)Ox quinary electrocatalyst with a high Ce content from 665 oxide compositions using a high-throughput method. This high-throughput method is herein a promising and powerful strategy to quickly optimize the ratios of various constituents, especially for those with multicomponents, but it is still far from general research studies because of its difficulty in the implementation. Thus, more methods and strategies are urgently needed to investigate and optimize the amount of RE elements required for excellent catalytic properties of these electrocatalysts.

(2) Investigations on the detailed structures of RE element–incorporated electrocatalysts during the electrochemical process. For most electrochemical reactions, RE element–based species are not catalytically active, in which they facilitated the active centers *via* different interactions. Learning the structural changes of RE element–based species during electrocatalysis can help in understanding the detailed reaction process. In particular, in situ techniques are favored to explore the changes of different catalytic sites here to clarify the reaction mechanism. However, few reports demonstrated the changes of structures and corresponding catalytic mechanisms with operando techniques in detail to reveal the roles of RE elements and compounds during different electrochemical processes [59,83,98]. In this regard, investigating the interaction between RE element species and other transition metals, the adsorption and conversion of intermediates on RE element species, and the dynamic changes in structures of electrocatalysts at different reaction paths in detail would facilitate the understanding of actual roles of RE elements in electrocatalysis.

(3) Insight into the catalytic mechanism of RE element–based electrocatalysts and their rational design. Although several reports have described the decent catalytic performance of RE element–based electrocatalysts without adding other active transition metals [67–70,84,95], the corresponding catalytic mechanisms as well as structural evolution and changes of electrocatalysts for these electrocatalytic reactions are still not very clear, especially in the view of combining theoretical investigations and operando analyses. Thus, lacking the knowledge of catalytic mechanisms is a great obstacle for the rational design of RE element–based and RE element–incorporated electrocatalysts.

(4) Developing highly active, multifunctional RE element–incorporated electrocatalysts. RE element incorporation can improve the activity of the original host for a specific reaction, although little research reported the multifunctional property of RE element–incorporated electrocatalysts with the enhancement of activity of various reactions simultaneously. For example, CeO_2-incorporated electrocatalysts were demonstrated to work as both anodic and cathodic materials with the remarkable activity and durability for full water electrolysis processes [34,49]. However, the multifunctional electrocatalysts and their applications in different processes are still lacking. As described previously, because RE element incorporation can promote the activity for OER, ORR, and MOR, using the RE element–incorporated electrocatalysts for ORR can also work as anodic materials for OER and MOR, and vice versa. Building such symmetric electrode structures would make the best of RE element–incorporated electrocatalysts, in which all these can substantially simplify the design and setups for practical applications, such as metal–air rechargeable batteries, DMFCs, and so on.

Conclusively, the exploration of RE element–incorporated electrocatalysts is rising rapidly over the past years and will be more attractive because of their fascinating chemical and electrocatalytic properties. However, what we have studied in this field of RE element–promoted electrocatalysis is still not enough to stride over the threshold of present challenges and problems, from the views of both science and practical applications. With the fast development of multidiscipline, both theoretical and experimental research studies are expected to combine together and shed light on the effects of RE elements, contributing to novel advances in electrocatalysis.

Acknowledgments

The authors acknowledge the financial support from the National Natural Science Foundation of China (Grant 21401148, 51672229) and the National 1000-Plan program. This work was also funded by

the Fundamental Research Funds for the Central Universities under Grants xjj2013102 and xjj2013043, the General Research Fund (CityU 11204618) of the Research Grants Council of Hong Kong SAR, China, and the Science Technology and Innovation Committee of Shenzhen Municipality (Grant JCYJ 20170818095520778). Prof. Qu is also supported by the Cyrus Tang Foundation through the Tang Scholar program.

Appendix A. Supplementary data

Supplementary data to this article can be found online at https://doi.org/10.1016/j.mtchem.2019.02.002.

References

[1] L. Han, S. Dong, E. Wang, Transition-metal (Co, Ni, and Fe)-based electrocatalysts for the water oxidation reaction, Adv. Mater. 9 (2016) 9266–9291.
[2] T. Tang, W.-J. Jiang, S. Niu, N. Liu, H. Luo, Y.-Y. Chen, S.-F. Jin, F. Gao, L.-J. Wan, J.-S. Hu, Electronic and morphological dual modulation of cobalt carbonate hydroxides by Mn doping toward highly efficient and stable bifunctional electrocatalysts for overall water splitting, J. Am. Chem. Soc. 139 (2017) 8320–8328.
[3] G. Wu, W. Chen, X. Zheng, D. He, Y. Luo, X. Wang, J. Yang, Y. Wu, W. Yan, Z. Zhuang, X. Hong, Y. Li, Hierarchical Fe-doped NiO_x nanotubes assembled from ultrathin nanosheets containing trivalent nickel for oxygen evolution reaction, Nanomater. Energy 38 (2017) 167–174.
[4] H. Wang, C. Tsai, D. Kong, K. Chan, F. Abild-Pedersen, J.K. Nørskov, Y. Cui, Transition-metal doped edge sites in vertically aligned MoS_2 catalysts for enhanced hydrogen evolution, Nano Res 8 (2015) 566–575.
[5] Q. Xiong, Y. Wang, P.-F. Liu, L.-R. Zheng, G. Wang, H.-G. Yang, P.-K. Wong, H. Zhang, H. Zhao, Cobalt covalent doping in MoS_2 to induce bifunctionality of overall water splitting, Adv. Mater. 30 (2018) 1801450.
[6] J. Su, R. Ge, K. Jiang, Y. Dong, F. Hao, Z. Tian, G. Chen, L. Chen, Assembling ultrasmall copper-doped rughenium oxide nanocrystals into hollow porous polyhedral: highly robust electrocatalysts for oxygen evolution in acidic media, Adv. Mater. 30 (2018) 1801351.
[7] J. Yu, W. Zhou, T. Xiong, A. Wang, S. Chen, B. Chu, Enhanced electrocatalytic activity of Co@N-doped carbon nanotubes by ultrasmall defect-rich TiO_2 nanoparticles for hydrogen evolution reaction, Nano Res 10 (2017) 2599–2609.
[8] J. Jiang, F. Sun, S. Zhou, W. Hu, H. Zhang, J. Dong, Z. Jiang, J. Zhao, J. Li, W. Yan, M. Wang, Atomic-level insight into super-efficient electrocatalytic oxygen evolution on iron and vanadium co-doped nickel (oxy)hydroxide, Nat. Commun. 9 (2018) 2885.
[9] M. Gong, W. Zhou, M.J. Kenney, R. Kapusta, S. Cowley, Y. Wu, B. Lu, M.-C. Lin, D.-Y. Wang, J. Yang, B.-J. Hwang, H. Dai, Blending Cr_2O_3 into a NiO-Ni electrocatalyst for sustained water splitting, Angew. Chem. Int. Ed. 54 (2015) 11989–11993.
[10] X. Liu, W. Xi, C. Li, X. Li, J. Shi, Y. Shen, J. He, L. Zhang, L. Xie, X. Sun, P. Wang, J. Luo, L.-M. Liu, Y. Ding, Nanoporous Zn-doped Co_3O_4 sheets with single-unite-cell-wide lateral surfaces for efficient oxygen evolution and water splitting, Nanomater. Energy 44 (2018) 371–377.
[11] M.H. Miles, Evaluation of electrocatalysts for water electrolysis in alkaline solutions, J. Electroanal. Chem. Interfac. 60 (1975) 89–96.
[12] T. Kitamura, C. Iwakura, H. Tamura, Hydrogen evolution at $LaNi_5$ and $MmNi_5$ electrode in alkaline solutions, Chem. Lett. 10 (1981) 965–966.
[13] H. Tamura, C. Iwakura, T. Kitamura, Hydrogen evolution at $LaNi_5$-type alloy electrodes, J. Less Common. Met. 89 (1983) 567–574.
[14] P. Hernandez-Fernandez, F. Masini, D.N. McCarthy, C.E. Strebel, D. Friebel, D. Deiana, P. Malacrida, A. Nierhoff, A. Bodin, A.M. Wise, J.H. Nielsen, T.W. Hansen, A. Nilsson, I.E.L. Stephens, I. Chorkendorff, Mass-selected nanoparticles of Pt_xY as model catalysts for oxygen electroreduction, Nat. Chem. 6 (2014) 732–738.
[15] F. Safizadeh, E. Ghali, G. Houlachi, Electrocatalysis developments for hydrogen evolution reaction in alkaline solutions-a review, Int. J. Hydrog. Energy 40 (2015) 256–274.
[16] M.M. Jakšić, Electrocatalysis of hydrogen evolution in the light of the Brewer-Engel theory for bonding in metals and intermetallic phases, Electrochim. Acta 29 (1984) 1539–1550.
[17] F. Rosalbino, G. Borzone, E. Angelini, R. Raggio, Hydrogen evolution reaction on Ni-RE (RE=rare earth) crystalline alloys, Electrochim. Acta 48 (2003) 3939–3944.
[18] D.S.P. Cardoso, L. Amaral, D.M.F. Santos, B. Šljukić, C.A.C. Sequeira, D. Macciò, A. Saccone, Enhancement of hydrogen evolution in alkaline water electrolysis by using nickel-rare earth alloys, Int. J. Hydrog. Energy 40 (2015) 4295–4302.
[19] M.A. Domínguez-Crespo, A.M. Torres-Huerta, B. Brachetti-Sibaja, A. Flores-Vela, Electrochemical performance of Ni-RE (RE=rare earth) as electrode material for hydrogen evolution reaction in alkaline medium, Int. J. Hydrog. Energy 36 (2011) 135–151.
[20] F. Rosalbino, D. Macciò, E. Angelini, A. Saccone, S. Delfino, Electrocatalytic properties of Fe-R (R=rare earth metal) crystalline alloys as hydrogen electrodes in alkaline water electrolysis, J. Alloy. Comp. 403 (2005) 275–282.
[21] F. Rosalbino, D. Macciò, E. Angelini, A. Saccone, S. Delfino, Characterization of Fe-Zn-R (R=rare earth metal) crystalline alloys as electrocatalysts for hydrogen evolution, Int. J. Hydrog. Energy 33 (2008) 2660–2667.
[22] F. Rosalbino, D. Macciò, A. Saccone, E. Angelini, S. Delfino, Fe-Mo-R (R=rare earth metal) crystalline alloys as cathode material for hydrogen evolution reaction in alkaline solution, Int. J. Hydrog. Energy 36 (2011) 1965–1973.
[23] D.M.F. Santos, C.A.C. Sequeira, D. Macciò, A. Saccone, J.L. Figueiredo, Platinum-rare earth electrodes for hydrogen evolution in alkaline water electrolysis, Int. J. Hydrog. Energy 38 (2013) 3137–3145.
[24] Z. Zheng, N. Li, C.-Q. Wang, D.-Y. Li, Y.-M. Zhu, G. Wu, Ni-CeO_2 composite cathode material for hydrogen evolution reaction in alkaline electrolyte, Int. J. Hydrog. Energy 37 (2012) 13921–13932.
[25] Z. Zheng, N. Li, C.-Q. Wang, D.-Y. Li, F.-Y. Meng, Y.-M. Zhu, Q. Li, G. Wu, Electrochemical synthesis of Ni-S/CeO_2 composite electrodes for hydrogen evolution reaction, J. Power Sources 230 (2013) 10–14.
[26] M. Zhao, H. Dong, Z. Chen, Z. Ma, L. Wang, G. Wang, W. Yang, G. Shao, Study of Ni-S/CeO_2 composite material for hydrogen evolution reaction in alkaline solution, Int. J. Hydrog. Energy 41 (2016) 20485–20493.
[27] M. Sheng, W. Weng, Y. Wang, Q. Wu, S. Hou, Co-W/CeO_2 composite coatings for highly active electrocatalysis of hydrogen evolution reaction, J. Alloy. Comp. 743 (2018) 682–690.
[28] Z. Weng, W. Liu, L.-C. Yin, R. Fang, M. Li, E.I. Altman, Q. Fan, F. Li, H.-M. Cheng, H. Wang, Metal/oxide interface nanostructures generated by surface segregation for electrocatalysis, Nano Lett. 15 (2015) 7704–7710.
[29] R. Zhang, X. Ren, S. Hao, R. Ge, Z. Liu, A.M. Asiri, L. Chen, Q. Zhang, X. Sun, Selective phosphidation: an effective strategy toward CoP/CeO_2 interface engineering for superior alkaline hydrogen evolution electrocatalysis, J. Mater. Chem. A 6 (2018) 1985–1990.
[30] L. Zhang, X. Ren, X. Guo, Z. Liu, A.M. Asiri, B. Li, L. Chen, X. Sun, Efficient hydrogen evolution electrocatalysis at alkaline pH by interface engineering of Ni_2P-CeO_2, Inorg. Chem. 57 (2018) 548–552.
[31] L. Xiong, J. Bi, L. Wang, S. Yang, Improving the electrocatalytic property of CoP for hydrogen evolution by constructing porous ternary CeO_2-CoP-C hybrid nanostructure via ionic exchange of MOF, Int. J. Hydrog. Energy 43 (2018) 20372–20381.
[32] Z. Sun, J. Zhang, J. Xie, X. Zheng, M. Wang, X. Li, B. Tang, High-performance alkaline hydrogen evolution electrocatalyzed by a Ni_3N-CeO_2 nanohybrid, Inorg. Chem. Front. 5 (2018) 3042–3045.
[33] X. Wang, Y. Yang, L. Diao, Y. Tang, F. He, E. Liu, C. He, C. Shi, J. Li, J. Sha, S. Ji, P. Zhang, L. Ma, N. Zhao, CeO_x-decorated NiFe-layered double hydroxide for efficient alkaline hydrogen evolution by oxygen vacancy engineering, ACS Appl. Mater. Interfaces 10 (2018) 35145–35153.
[34] E. Demir, S. Akbayrak, A.M. Önal, S. Özkar, Nanoceria-supported ruthenium(0) nanoparticles: highly active and stable catalysts for hydrogen evolution from water, ACS Appl. Mater. Interfaces 10 (2018) 6299–6308.
[35] X. Long, H. Lin, D. Zhou, Y. An, S. Yang, Enhancing full water-splitting performance of transition metal bifunctional electrocatalysts in alkaline solutions by tailoring CeO_2-transition metal oxides-Ni nanointerfaces, ACS Energy Lett 3 (2018) 290–296.
[36] W. Gao, M. Yan, H.-Y. Cheung, Z. Xia, X. Zhou, Y. Qin, C.-Y. Wong, J.C. Ho, C.-R. Chang, Y. Qu, Modulating electronic structure of CoP electrocatalysts towards enhanced hydrogen evolution by Ce chemical doping in both acidic and basic media, Nanomater. Energy 38 (2017) 290–296.
[37] Y. Liu, X. Lu, Z. Che, C. Zhang, M. Han, J. Bao, Z. Dai, Amorphous $Y(OH)_3$-promoted Ru/$Y(OH)_3$ nanohybrids with high durability for electrocatalytic hydrogen evolution in alkaline media, Chem. Commun. 54 (2018) 12202–12205.
[38] T. Reier, H.N. Nong, D. Teschner, R. Schlögl, P. Strasser, Electrocatalytic oxygen evolution reaction in acidic environments-reaction mechanisms and catalysts, Adv. Energy Mater. 7 (2017) 1601275.
[39] J.W.D. Ng, M. García-Melchor, M. Bajdich, P. Chakthranont, C. Kirk, A. Vojvodic, T.F. Jaramillo, Gold-supported cerium-doped NiO_x catalysts for water oxidation, Nat. Energy 1 (2016) 16053.
[40] H. Xu, B. Wang, C. Shan, P. Xi, W. Liu, Y. Tang, Ce-doped NiFe-layered double hydroxide ultrathin nanosheets/nanocarbon hierarchical nanocomposite as an efficient oxygen evolution catalyst, ACS Appl. Mater. Interfaces 10 (2018) 6336–6345.
[41] Y. Ma, W. Gao, Z. Zhang, S. Zhang, Z. Tian, Y. Liu, J.C. Ho, Y. Qu, Regulating the surface of nanoceria and its applications in heterogeneous catalysis, Surf. Sci. Rep. 73 (2018) 1–36.
[42] Y.-R. Zheng, M.-R. Gao, Q. Gao, H.-H. Li, J. Xu, Z.-Y. Wu, S.-H. Yu, An efficient CeO_2/$CoSe_2$ nanobelt composite for electrochemical water oxidation, Small 11 (2015) 182–188.
[43] J.-X. Feng, S.-H. Ye, H. Xu, Y.-X. Tong, G.-R. Li, Design and synthesis of FeOOH/CeO_2 heterolayered nanotube electrocatalysts for the oxygen evolution reaction, Adv. Mater. 28 (2016) 4698–4703.
[44] D.-J. Li, Z.-G. Gu, W. Zhang, Y. Kang, J. Zhang, Epitaxial encapsulation of homodispersed CeO_2 in a cobalt-porphyrin network derived thin film for the highly efficient oxygen evolution reaction, J. Mater. Chem. A 5 (2017) 20126–20130.
[45] Z. Liu, N. Li, H. Zhao, Y. Zhang, Y. Huang, Z. Yin, Y. Du, Regulating active species of $Ni(OH)_2$ by CeO_2: 3D CeO_2/$Ni(OH)_2$/carbon foam as an efficient electrode for oxygen evolution reaction, Chem. Sci. 8 (2017) 3211–3217.
[46] T. Odedairo, X. Yan, X. Yao, K. Ostrikov, Z. Zhu, Hexagonal sphericon hematite with high performance for water oxidation, Adv. Mater. 29 (2017) 1703792.

[47] J.-H. Kim, K. Shin, K. Kawashima, D.H. Youn, J. Lin, T.E. Hong, Y. Liu, B.R. Wygant, J. Wang, G. henkelman, C.B. Mullins, Enhanced activity promoted by CeO_x on a CoO_x electrocatalyst for the oxygen evolution reaction, ACS Catal. 8 (2018) 4257–4265.

[48] H. Xu, J. Cao, C. Shan, B. Wang, P. Xi, W. Liu, Y. Tang, MOF-derived hollow CoS decorated with CeO_x nanoparticles for boosting oxygen evolution reaction electrocatalysis, Angew. Chem. Int. Ed. 130 (2018) 8790–8794.

[49] W. Gao, Z. Xia, F. Cao, J.C. Ho, Z. Jiang, Y. Qu, Comprehensive understanding of the spatial configurations of CeO_2 in NiO for the electrocatalytic oxygen evolution reaction: embed or surface-loaded, Adv. Funct. Mater. 28 (2018) 1706056.

[50] D. Zhao, Y. Pi, Q. Shao, Y. Feng, Y. Zhang, X. Huang, Enhancing oxygen evolution electrocatalysis via the intimate hydroxide-oxide interface, ACS Nano 12 (2018) 6245–6251.

[51] M.F. Montemor, Functional and smart coatings for corrosion protection: a review of recent advances, Surf. Coating. Technol. 258 (2014) 17–37.

[52] K. Obata, K. Tkanabe, A permselective CeO_x coating to improve the stability of oxygen evolution electrocatalysts, Angew. Chem. 130 (2018) 1632–1636.

[53] J. Greeley, I.E.L. Stephens, A.S. Bondarenko, T.P. Johansson, H.A. Hansen, T.F. Jaramillo, J. Rossmeisl, I. Chorkendorff, J.K. Nørskov, Alloys of platinum and early transition metals as oxygen reduction electrocatalysts, Nat. Chem. 1 (2009) 552–556.

[54] A. Velázquez-Palenzuela, F. Masini, A.F. Pedersen, M. Escudero-Escribano, D. Deiana, P. Malacrida, T.W. Hansen, D. Friebel, A. Nilsson, I.E.L. Stephens, I. Chorkendorff, The enhanced activity of mass-selected Pt_xGd nanoparticles for oxygen reduction, J. Catal. 328 (2015) 297–307.

[55] A.F. Pedersen, E.T. Ulrikkeholm, M. Escudero-Escribano, T.P. Johansson, P. Malacrida, C.M. Pedersen, M.H. Hansen, K.D. Jensen, J. Rossmeisl, D. Friebel, A. Nilsson, I. Chorkendorff, I.E.L. Stephens, Probing the nanoscale structure of the catalytically active overlayer on Pt alloys with rare earths, Nanomater. Energy 29 (2016) 249–260.

[56] M. Escudero-Escribano, P. Malacrida, M.H. Hansen, U.G. Vej-Hansen, A. Velázquez-Palenzuela, V. Tripkovic, J. Schiøtz, j. Rossmeisl, I.E.L. Stephens, I. Chorkendorff, Tuning the activity of Pt alloy electrocatalysts by means of the lanthanide contraction, Science 352 (2016) 73–76.

[57] C.-W. Liu, Y.-C. Wei, K.-W. Wang, Surface condition manipulation and oxygen reduction enhancement of PtAu/C catalysts synergistically modified by CeO_2 addition and N_2 treatment, J. Phys. Chem. C 115 (2011) 8702–8708.

[58] Y. Luo, L. Calvillo, C. Daiguebonne, M.K. Daletou, G. Granozzi, N. Alonso-Vante, A highly efficient and stable oxygen reduction reaction on $Pt/CeO_x/C$ electrocatalyst obtained via a sacrificial precursor based on a metal-organic framework, Appl. Catal. B Environ. 189 (2016) 39–50.

[59] A.B. Yousaf, M. Imran, N. Uwitonze, A. Zeb, S.J. Zaidi, T.M. Ansari, G. Yasmeen, S. Manzoor, Enhanced electrocatalytic performance of Pt_3Pd_1 alloys supported on CeO_2/C for methanol oxidation and oxygen reduction reactions, J. Phys. Chem. C 121 (2017) 2069–2079.

[60] F. Xu, D. Wang, B. Sa, Y. Yu, S. Mu, One-pot synthesis of $Pt/CeO_2/C$ catalyst for improving the ORR activity and durability of PEMFC, Int. J. Hydrog. Energy 42 (2017) 13011–13019.

[61] T. Masuda, H. Fukumitsu, K. Fugane, H. Togasaki, D. Matsumura, K. Tamura, Y. Nishihata, H. Yoshikawa, K. Kobayashi, T. Mori, K. Uosaki, Role of cerium oxide in the enhancement of activity for the oxygen reduction reaction at $Pt-CeO_x$ nanocomposite electrocatalyst-an in situ electrochemical X-ray adsorption fine structure study, J. Phys. Chem. C 116 (2012) 10098–10102.

[62] Y. Li, X. Zhang, S. Wang, G. Sun, Durable platinum-based electrocatalyst supported by multiwall carbon nanotubes modified with CeO_2, ChemElectrochem 5 (2018) 2442–2448.

[63] K. Liu, X. Huang, H. Wang, F. Li, Y. Tang, J. Li, M. Shao, Co_3O_4-CeO_2/C as a highly active electrocatalyst for oxygen reduction reaction in Al-air batteries, ACS Appl. Mater. Interfaces 8 (2016) 34422–34430.

[64] H. Wei, X. Su, J. Liu, J. Tian, Z. Wang, K. Sun, Z. Rui, W. Yang, Z. Zou, A CeO_2 modified phenylenediamine-based Fe/N/C with enhanced durability/stability as non-precious metal catalyst for oxygen reduction reaction, Electrochem. Commun. 88 (2018) 19–23.

[65] W. Xia, J. Li, T. Wang, L. Song, H. Guo, H. Gong, C. Jiang, B. Gao, J. He, The synergistic effect of ceria and Co in N-doped leaf-like carbon nanosheets derived from a 2D MOF and their enhanced performance in the oxygen reduction reaction, Chem. Commun. 54 (2018) 1623–1626.

[66] A. Sivanantham, P. Ganesan, S. Shanmugam, A synergistic effect of Co and CeO_2 in nitrogen-doped carbon nanostructure for the enhanced oxygen electrode activity and stability, Appl. Catal. B Environ. 237 (2018) 1148–1159.

[67] X. Yuan, H. Ge, X. Liu, X. Wang, W. Chen, W. Dong, F. Huang, Efficient catalyst of defective CeO_{2-x} and few-layer carbon hybrid for oxygen reduction reaction, J. Alloy. Comp. 688 (2016) 613–618.

[68] L. Yang, Z. Cai, L. Hao, Z. Xing, Y. Dai, X. Xu, S. Pan, Y. Duan, J. Zou, Nano Ce_2O_2S with highly enriched oxygen-defecient Ce^{3+} sites supported by N and S dual-doped carbon as an active oxygen-supply catalyst for the oxygen reduction reaction, ACS Appl. Mater. Interfaces 9 (2017) 22519–22529.

[69] L. Sun, L. Zhou, C. Yang, Y. Yuan, CeO_2 nanoparticle-decorated reduced graphene oxide as an efficient bifunctional electrocatalyst for oxygen reduction and evolution reactions, Int. J. Hydrog. Energy 42 (2017) 15140–15148.

[70] Y. Yu, B. He, Y. Liao, X. Yu, Z. Mu, Y. Xing, S. Xing, Preparation of hollow CeO_2/$CePO_4$ with nitrogen and phosphorous co-doped carbon shells for enhanced oxygen reduction reaction catalytic activity, ChemElectroChem 5 (2018) 793–798.

[71] J. Wang, J. Xi, Y. Bai, Y. Shen, J. Sun, L. Chen, W. Zhu, X. Qiu, Structural designing of Pt-CeO_2-CNTs for methanol electro-oxidation, J. Power Sources 164 (2007) 555–560.

[72] Z. Sun, X. Wang, Z. Liu, H. Zhang, P. Yu, L. Mao, Pt-Ru/CeO_2/carbon nanotube nanocomposites: an efficient electrocatalyst for direct methanol fuel cells, Langmuir 26 (2010) 12383–12389.

[73] E. Lee, A. Manthiram, One-step reverse microemulsion synthesis of Pt-CeO_2/C catalysts with improved nanomorphology and their effect on methanol electrooxidation reaction, J. Phys. Chem. C 114 (2010) 21833–21839.

[74] Y. Zhou, Y. Gao, Y. Liu, J. Liu, High efficiency Pt-CeO_2/carbon nanotubes hybrid composite as an anode electrocatalyst for direct methanol fuel cells, J. Power Sources 195 (2010) 1605–1609.

[75] D.-J. Guo, Z.-H. Jing, A novel co-precipitation method for preparation of Pt-CeO_2 composites on multi-walled carbon nanotubes for direct methanol fuel cells, J. Power Sources 195 (2010) 3802–3805.

[76] D.R. Ou, T. Mori, H. Togasaki, M. Takahashi, F. Ye, J. Drennan, Microstructural and metal-support interaction of the Pt-CeO_2/C catalysts for direct methanol fuel cell application, Langmuir 27 (2011) 3859–3866.

[77] Y.-Y. Chu, Z.-B. Wang, Z.-Z. Jiang, D.-M. Gu, G.-P. Yin, A novel structural design of a Pt/C-CeO_2 catalyst with improved performance for methanol electro-oxidation by β-cyclodextrin carbonization, Adv. Mater. 23 (2011) 3100–3104.

[78] D.-M. Gu, Y.-Y. Chu, Z.-B. Wang, Z.-Z. Jiang, G.-P. Yin, Y. Liu, Methanol oxidation on Pt/CeO_2-C electrocatalyst prepared by microwave-assisted ethylene glycol process, Appl. Catal. B Environ. 102 (2011) 9–18.

[79] X. Yu, L. Kuai, B. Geng, CeO_2/rGO/Pt sandwich nanostructure: rGO-enhanced electron transmission between metal oxide and metal nanoparticles for anodic methanol oxidation of direct methanol fuel cells, Nanoscale 4 (2012) 5738–5743.

[80] S.K. Meher, G.R. Rao, Polymer-assisted hydrothermal synthesis of highly reducible shuttle-shaped CeO_2: microstructural effect on promoting Pt/C for methanol electrooxidation, ACS Catal. 2 (2012) 2795–2809.

[81] S. Yu, Q. Liu, W. Yang, K. Han, Z. Wang, H. Zhu, Graphene-CeO_2 hybrid support for Pt nanoparticles as potential electrocatalyst for direct methanol fuel cells, Electrochim, Acta 94 (2013) 245–251.

[82] H. Xu, A.-L. Wang, Y.-X. Tong, G.-R. Li, Enhanced catalytic activity and stability of Pt/CeO_2/PANI hybrid hollow nanorod arrays for methanol electro-oxidation, ACS Catal. 6 (2016) 5198–5206.

[83] O. Brummel, F. Waidhas, F. Faisal, R. Fiala, M. Vorokhta, I. Khalakhan, M. Dubau, A. Figueroba, G. Kovács, H.A. Aledsandrov, G.N. Vayssilov, S.M. Kozlov, K.M. Neyman, V. Matolín, J. Jibuda, Stabilization of small platinum nanoparticles on Pt-CeO_2 thin film electrocatalysts during methanol oxidation, J. Phys. Chem. C 120 (2016) 19723–19736.

[84] B. Kaur, R. Srivastava, B. Satpati, Highly efficient CeO_2 decorated nano-ZSM-5 catalyst for electrochemical oxidation of methanol, ACS Catal. 6 (2016) 2654–2663.

[85] C. Xu, P.K. Shen, Novel Pt/CeO_2/C catalysts for electrooxidation of alcohols in alkaline media, Chem. Commun. 19 (2004) 2238–2239.

[86] C. Xu, P.K. Shen, Electrochemical oxidation of ethanol on Pt-CeO_2/C catalysts, J. Power Sources 142 (2005) 27–29.

[87] Y. Bai, J. Wu, X. Qiu, J. Xi, J. Wang, J. Li, W. Zhu, L. Chen, Electrochemical characterization of Pt-CeO_2/C and Pt-$Ce_xZr_{1-x}O_2/C$ catalysts for ethanol electro-oxidation, Appl. Catal. B Environ. 73 (2007) 144–149.

[88] Y.-C. Wei, C.-W. Liu, W.-D. Kang, C.-M. Lai, L.-D. Tsai, K.-W. Wang, Electrocatalytic activity enhancement of Pd-Ni electrocatalysts for the ethanol electro-oxidation in alkaline medium: the promotional effect of CeO_2 addition, J. Electroanal. Chem. 660 (2011) 64–70.

[89] Y. Wang, S. Wang, X. Wang, CeO_2 promoted electro-oxidation of formic acid on Pd/C nano-electrocatalysts, Electrochem. Solid State Lett. 12 (2009) B73–B76.

[90] M. Srivastava, A.K. Das, P. Khanra, M.E. Uddin, N.H. Kim, J.H. Lee, Characterizations of in situ grown ceria nanoparticles on reduced graphene oxide as a catalyst for the electrooxidation of hydrazine, J. Mater. Chem. A 1 (2013) 9792–9801.

[91] Y. Katayama, T. Okanishi, H. Muroyama, T. Matsui, K. Eguchi, Electrochemical oxidation of ammonia over rare earth oxide modified platinum catalysts, J. Phys. Chem. C 119 (2015) 9134–9141.

[92] D. Gao, Y. Zhang, Z. Zhou, F. Cai, X. Zhao, W. Huang, Y. Li, J. Zhu, P. Liu, F. Yang, G. Wang, X. Bao, Enhancing CO_2 electroreduction with the metal-oxide interface, J. Am. Chem. Soc. 139 (2017) 5652–5655.

[93] Y. Wang, Z. Chen, P. Han, Y. Du, Z. Gu, X. Xu, G. Zheng, Single-atomic Cu with multiple oxygen vacancies on ceria for electrocatalytic CO_2 reduction to CH_4, ACS Catal. 8 (2018) 7113–7119.

[94] C. Lv, C. Yan, G. Chen, D. Yu, J. Sun, Y. Zhou, G. Yu, An amorphous noble-metal-free electrocatalyst enables N_2 fixation under ambient conditions, Angew. Chem. 130 (2018) 6181–6184.

[95] X. Li, L. Li, X. Ren, D. Wu, Y. Zhang, H. Ma, X. Sun, B. Du, Q. Wei, B. Li, Enabling electrocatalytic N_2 reduction to NH_3 by Y_2O_3 nanosheet under ambient conditions, Ind. Eng. Chem. Res. 57 (2018) 16622–16627.

[96] J.A. Haber, C. Xiang, D. Guevarra, S. Jung, J. Jin, J.M. Gregoire, High-throughput mapping of the electrochemical properties of $(Ni-Fe-Co-Ce)O_x$ oxygen-evolution catalysts, ChemElectroChem 1 (2014) 524–528.

[97] J.A. Haber, E. Anzenburg, J. Yano, C. Kisielowski, J.M. Gregoire, Multiphase nanostructure of a quinary metal oxide electrocatalyst reveals a new direction for OER electrocatalyst design, Adv. Energy Mater. 5 (2015) 1402307.

[98] M. Favaro, W.S. Drisdell, M.A. Marcus, J.M. Gregoire, E.J. Crumlin, J.A. Haber, J. Yano, An operando investigation of $(Ni-Fe-Co-Ce)O_x$ system as highly efficient electrocatalyst for oxygen evolution reaction, ACS Catal. 7 (2017) 1248–1258.